Check for updates

Abscisic Acid-Induced Reactive Oxygen Species Are Modulated by Flavonols to Control Stomata Aperture[1][OPEN]

Justin M. Watkins, Jordan M. Chapman, and Gloria K. Muday[2]

Wake Forest University, Department of Biology and Center for Molecular Signaling, Winston-Salem, North Carolina 27109

ORCID IDs: 0000-0003-4127-1950 (J.M.W.); 0000-0001-6755-9341 (J.M.C.); 0000-0002-0377-4517 (G.K.M.).

Abscisic acid (ABA) increases reactive oxygen species (ROS) in guard cells to close Arabidopsis (*Arabidopsis thaliana*) stomata. In tomato (*Solanum lycopersicum*), we find that ABA-increased ROS is followed by stomatal closure and that both responses are blocked by inhibitors of ROS-producing respiratory burst oxidase enzymes. ABA-induced ROS sensor fluorescence accumulates in the nucleus, chloroplasts, and endomembranes. The accumulation of flavonol antioxidants in guard cells, but not surrounding pavement cells, was visualized by confocal microscopy using a flavonol-specific fluorescent dye. Decreased flavonols in guard cells in the *anthocyanin reduced* (*are*) mutant and elevated levels in the *anthocyanin without* (*aw*) mutant were quantified by confocal microscopy and in leaf extracts by mass spectrometry. Consistent with flavonols acting as antioxidants, higher levels of ROS were detected in guard cells of the tomato *are* mutant and lower levels were detected in *aw* both at homeostasis and after treatment with ABA. These results demonstrate the inverse relationship between flavonols and ROS. Guard cells of *are* show greater ABA-induced closure than the wild type, reduced light-dependent guard cell opening, and reduced water loss, with *aw* having opposite responses. Ethylene treatment of wild-type tomato plants increased flavonol accumulation in guard cells; however, no flavonol increases were observed in *Neverripe* (*Nr*), an ethylene receptor mutant. Consistent with lower levels of ROS due to elevated flavonols, ethylene treatments decreased ABA-induced stomatal closure in the wild type, but not *Nr*, with ethylene responses attenuated in the *are* mutant. Together, these results are consistent with flavonols dampening the ABA-dependent ROS burst that drives stomatal closure and facilitating stomatal opening to modulate leaf gas exchange.

Reactive oxygen species (ROS) have historically been considered damaging agents within cells; however, recent studies have demonstrated that these molecules also serve as second messengers in signaling pathways (Gilroy et al., 2016; Choudhury et al., 2017). ROS signals control plant growth and development, including gravitropism (Cervantes, 2001; Joo et al., 2001), guard cell physiology (Mittler and Blumwald, 2015; Sierla et al., 2016; Singh et al., 2017), and modulation of root architecture (Foreman et al., 2003; Maloney et al., 2014; Li et al., 2015; Orman-Ligeza et al., 2016). The reactive nature of ROS allows these compounds to function as signaling molecules by reversibly oxidizing Cys residues in proteins, modulating enzyme structure or activity (Poole et al., 2004; Poole and Nelson, 2008; Choudhury et al., 2017). If ROS reach damaging levels within the cell, the resulting oxidative stress can cause irreversible oxidative modifications of proteins, DNA molecules, and membranes (Mittler, 2002; Asada, 2006; Van Breusegem and Dat, 2006; Choudhury et al., 2017). Therefore, ROS homeostasis is highly regulated in plant cells by enzymatic and small-molecule antioxidants, such as ascorbic acid, glutathione, and flavonoids (Rice-Evans et al., 1997; Heim et al., 2002; Sharma et al., 2012; Baxter et al., 2014; Inupakutika et al., 2016; Singh et al., 2016). This work explores the role of flavonol antioxidants in modulating signaling-induced ROS in guard cells.

In both plants and animals, ROS can be generated by respiratory burst oxidases (RBOH)/NADPH oxidase enzymes, which reside in the plasma membrane (Mustilli et al., 2002; Yoshida et al., 2002; Swanson and Gilroy, 2010). RBOH produces superoxide, which can be converted spontaneously or enzymatically into hydrogen peroxide (H_2O_2; Steinhorst and Kudla, 2013). The activity of RBOH is induced by hormones, such as ABA

[1] This project was supported by the USDA National Institute of Food and Agriculture program and the Agriculture and Food Research Initiative in a predoctoral fellowship (2014-67011-22277 to J.M.W.) and a foundational grant (2015-06811 to G.K.M.). The work was also supported by a WFU Center for Molecular Signaling Graduate Fellowship to J.M.W. The National Science Foundation supported the purchase of the laser scanning confocal microscope (NSF-MRI-0722926 and MRI-1039755) and the purchase of an Orbitrap Mass Spectrometer (MRI-947028)

[2] Address correspondence to muday@wfu.edu.

The author responsible for distribution of materials integral to the findings presented in this article in accordance with the policy described in the Instructions for Authors (www.plantphysiol.org) is: Gloria K. Muday (muday@wfu.edu).

J.M.W. and G.K.M. conceived the research plan and designed experiments; J.M.W. performed all the guard cell experiments and data analysis; J.M.C. performed the flavonol quantification; J.M.W. wrote the article with contributions of all the authors; G.K.M. supervised the project and provided editorial input into the writing.

[OPEN] Articles can be viewed without a subscription.

www.plantphysiol.org/cgi/doi/10.1104/pp.17.01010

 © 2017 American Society of Plant Biologists. All Rights Reserved.

(Pei et al., 2000; Jiang and Zhang, 2002), and abiotic stress, such as high light (Karpiński et al., 2013). ROS produced by RBOH have been shown to function in numerous signaling pathways in Arabidopsis (*Arabidopsis thaliana*), due to the availability of null mutants in genes encoding RBOH enzymes (Suzuki et al., 2011). These mutants have been used to demonstrate the importance of a ROS burst in guard cell signaling (Kwak et al., 2003; Chater et al., 2015).

RBOH production of ROS in guard cells occurs in response to ABA signaling, triggering a complex signaling cascade to close stomata (Assmann and Jegla, 2016; Balmant et al., 2016; Jezek and Blatt, 2017). In response to environmental stress, such as drought, ABA levels increase in guard cells, where they bind to a soluble receptor to trigger stomatal closure (Hornberg and Weiler, 1984; McCourt and Creelman, 2008). The activated ABA receptor inhibits protein phosphatases, resulting in the increased activity of several enzymes, including RBOHs, as a result of enhanced phosphorylation (Mustilli et al., 2002; Yoshida et al., 2002; Ma et al., 2009; Park et al., 2009). RBOH activation results in a transient burst of ROS in guard cells (Pei et al., 2000; Jiang and Zhang, 2003; Sierla et al., 2016). The ROS burst opens calcium ion influx channels (McAinsh et al., 1996; Allen et al., 2000; Blatt et al., 2007; Mittler and Blumwald, 2015; Minguet-Parramona et al., 2016), which, in turn, activate ion efflux channels on the plasma membrane. These ion concentration changes lead to the efflux of water, so guard cells become flaccid, causing stomatal closure (Hedrich et al., 1990; Schroeder and Hagiwara, 1990; Chen et al., 2010; Wang et al., 2013).

Plant cells employ multiple mechanisms to regulate the levels of ROS to modulate signaling and prevent oxidative stress. One mechanism is the synthesis of flavonol metabolites that function as antioxidants in vitro (Rice-Evans et al., 1997; Gayomba et al., 2017) and have been shown to modulate ROS-regulated root growth in tomato (*Solanum lycopersicum*; Maloney et al., 2014) and guard cell signaling in Arabidopsis (Watkins et al., 2014; An et al., 2016). Flavonols are early intermediates in the flavonoid biosynthetic pathway, which gives rise to a variety of important specialized metabolites (Winkel-Shirley, 2001; Buer et al., 2010). Figure 1 contains a diagram of this flavonoid biosynthesis pathway in Arabidopsis and tomato (Winkel-Shirley, 2001; Lepiniec et al., 2006). Tomato plants accumulate high levels of two flavonols, kaempferol and quercetin, and several others, which can be decorated with a diversity of carbohydrate modifications (Ballester et al., 2010). Mutants with defects in flavonol synthesis have helped define the pathway and can be used to understand how tomato guard cells regulate flavonol antioxidant synthesis to modulate levels of ROS in this important crop species.

Rapid and profound changes in flavonol accumulation can occur in response to changing environmental parameters and growth and developmental signals (Winkel-Shirley, 2002; Gayomba et al., 2017). Environmental stress, such as high light and drought, can cause increased synthesis of flavonols, providing an important

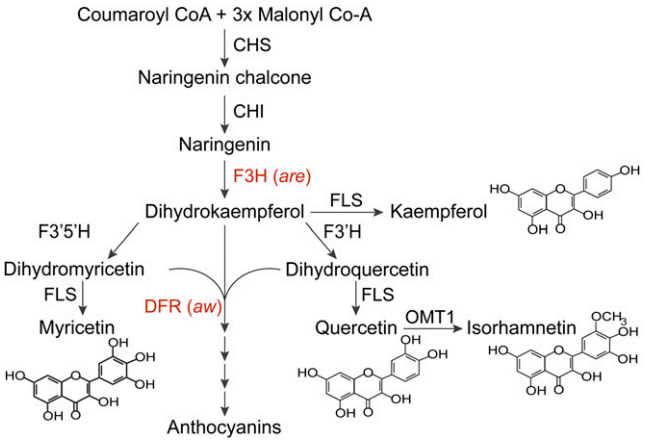

Figure 1. The flavonol biosynthetic pathway in tomato is illustrated, showing enzymatic steps and indicating tomato anthocyanin mutant names. ANS, Anthocyanidin synthase; CHI, chalcone isomerase; CHS, chalcone synthase; DFR, dihydroflavonol reductase; F3H, flavanone 3-hydroxylase; F3′H, flavonoid 3′-hydroxylase; F3′5′H, flavonoid 3′,5′-hydroxylase; FLS, flavonol synthase; OMT1, flavone 3′-*O*-methyltransferase 1. Tomato mutants are *anthocyanin reduced* (*are*) and *anthocyanin without* (*aw*). This figure is modified from Gayomba et al. (2017).

mechanism to control stress-induced ROS synthesis (Tattini et al., 2004; Lepiniec et al., 2006; Hichri et al., 2011). This pathway also is hormonally regulated; auxin and ethylene have been shown to increase flavonol synthesis through changes in expression of the genes encoding pathway enzymes (Buer et al., 2010; Lewis et al., 2011). Ethylene-induced flavonol synthesis reduced ROS in Arabidopsis guard cells, altering stomatal closure (Watkins et al., 2014).

The role of ROS signaling in guard cells is well established in Arabidopsis (Mittler and Blumwald, 2015; Sierla et al., 2016; Singh et al., 2016), but less is known about these signaling molecules and their regulation in agricultural species because of the limited number of mutants that have altered ROS homeostasis. Given the essential function of guard cells in regulating gas exchange and water loss, a better understanding of how crop plants mediate ROS signaling is essential to improving crop health, productivity, and ability to deal with stressful growth environments. In tomato guard cells, increases in ROS accumulation in response to pathogen infections (Lee et al., 1999), hormone signaling (Xia et al., 2014; Farber et al., 2016), and CO_2 concentrations (Shi et al., 2015; Yi et al., 2015) have been linked to stomatal closure; however, it is not clear that guard cell closure in this species works through an ABA-induced ROS burst, as observed in Arabidopsis. Additionally, the antioxidant networks in tomato guard cells that regulate ROS signaling remain uncharacterized.

This study examined the role of ROS signaling in modulating stomatal closure in the important agricultural species of tomato. ABA-induced ROS bursts were shown to precede and be required for stomatal closure in wild-type guard cells and to have distinct localizations within these cells. Flavonol antioxidants accumulate in tomato

guard cells but were not detected in surrounding pavement cells. To test the function of flavonols in tomato guard cells, mutants with both elevated and depleted levels of flavonols, but with similar changes in early and late pathway intermediates, were examined. An inverse relationship between flavonols and ROS was observed in tomato mutants, which resulted in altered stomata closure in response to ABA and stomata opening in response to light. Altered flavonol levels in mutant guard cells were accompanied by altered water loss in whole leaves, consistent with flavonols modulating ABA-dependent stomatal closure. Treatment of seedlings with ethylene resulted in significant increases in flavonols in the wild type but not in an ethylene signaling mutant, *Neverripe* (*Nr*). This hormonal elevation of flavonols, like mutants with elevated flavonols, reduced ROS levels and altered ABA-dependent guard cell closure. These results showed that altering levels of flavonol antioxidants in guard cells through hormone treatment or mutations in flavonol biosynthesis alters ABA-dependent ROS accumulation and stomatal closure.

RESULTS

Guard Cells Show Localized Signal from ROS Sensors

To determine the role of ROS in tomato guard cell signaling, we optimized methods for the visualization of ROS using two ROS sensors. Fluorescence intensity of the oxidized ROS sensor CM 2′,7′-dihydrodichlorofluorescein diacetate (CM H_2DCF-DA; Halliwell and Whiteman, 2004; Swanson et al., 2011) was quantified by laser scanning confocal microscopy (LSCM). This sensor reports intracellular ROS, as it crosses the plasma membrane and the diacetate functional group is cleaved by intracellular esterases, trapping CM H_2DCF in cells. The settings used to image DCF were carefully defined to separate the chlorophyll autofluorescent signal from DCF in leaf peels isolated from the basal surface of tomato leaves. Figure 2A shows the DCF channel alone (green) and the overlay of DCF on top of the chlorophyll signal (magenta). DCF fluorescence was brightest in the nucleus, with this localization verified by Hoechst fluorescence, which overlaps this DCF signal (Supplemental Fig. S1), but also was observed in punctate structures that resembled endomembranes and in or overlaying chloroplasts.

In contrast to the uniform DCF fluorescence in the nucleus, the chloroplast-associated DCF signal is uneven, as is evident in the pink, green, and white signals associated with the chloroplast. To resolve this complex pattern, we examined the individual slices from Z-stacks and performed a colocalization analysis on the maximum intensity projections (Supplemental Fig. S2). It is clear from individual Z-slices that much of the DCF signal surrounds the chloroplast, while other parts of the signal are inside chloroplasts. We sampled a region of the nucleus and three guard cell chloroplasts and used the ZEN colocalization module. The resulting graphs of pixel intensity from the chlorophyll and DCF channels plotted on each axis were generated from three chloroplasts and the nucleus. DCF and chlorophyll signals in the nucleus do not colocalize (weighted colocalization coefficient of 0), while the majority of the pixels in the three chloroplast regions of interests contain both DCF and chlorophyll signal (weighted colocalization coefficients of 1, 0.96, and 0.78, respectively), consistent with DCF signal dispersed throughout the chloroplast and in what appear to be endomembrane regions of the guard cells. This level of resolution is beyond prior reports in Arabidopsis guard cells (Kwak et al., 2003; Watkins et al., 2014; Arnaud et al., 2017; Wu et al., 2017), suggesting important subcellular localization of ROS synthesis, which can now be revealed with new LSCM imaging capability. It is important to note that the presence of fluorescence indicates that oxidized DCF accumulates in specific subcellular locations, which is consistent with DCF diffusion into the distinct compartments followed by oxidization by local ROS. It is also possible that localized signal is due to dye permeability and localized sequestration.

To complement the DCF imaging experiments and to further define which ROS are accumulating in guard cells, we used a second dye, Peroxy Orange1 (PO1). PO1 has different structural and chemical characteristics, which make this more reactive with H_2O_2 and define dye uptake, accumulation, and sequestration (Dickinson et al., 2010). The settings used to image PO1 were carefully defined to separate the chlorophyll autofluorescent signal from PO1 in leaf peels isolated from the basal surface of tomato leaves (Fig. 2B). The patterns of PO1 accumulation mirror those of DCF, with signal in the nucleus, chloroplast, and cytoplasmic puncta. This similar pattern with two different ROS sensors strengthens the possibility that we are detecting localized ROS accumulation.

ABA-Induced ROS Accumulation in Tomato Guard Cells Is Required for Stomatal Closure

We used two approaches to examine the connection between RBOH-produced ROS and stomatal closure in tomato. First, we compared the kinetics of ABA-induced ROS generation with ABA-induced stomatal closure. Whole wild-type leaves were excised and placed in a stomatal opening buffer for 3 h under white light followed by incubation with 20 μM ABA for 0, 15, 30, and 45 min. ABA treatment increased DCF fluorescence to 2-fold higher than starting levels by the end of the 45-min time course after ABA treatment (Fig. 2, C and D). The increase in fluorescence in the entire guard cell was quantified, and all time points were significantly different from the time-0 control, as determined using two-way ANOVA followed by Tukey's posthoc test in at least 70 guard cells per time point over two separate experiments. The DCF fluorescence is stable across this time course in a mock-treated sample, with average fluorescence of 10,342 versus 10,513 after 0- and 45-min incubations, respectively.

We also quantified subcellular increases in DCF fluorescence after ABA treatment. Signal is elevated in the nucleus, overlaying chloroplasts, and most strikingly in

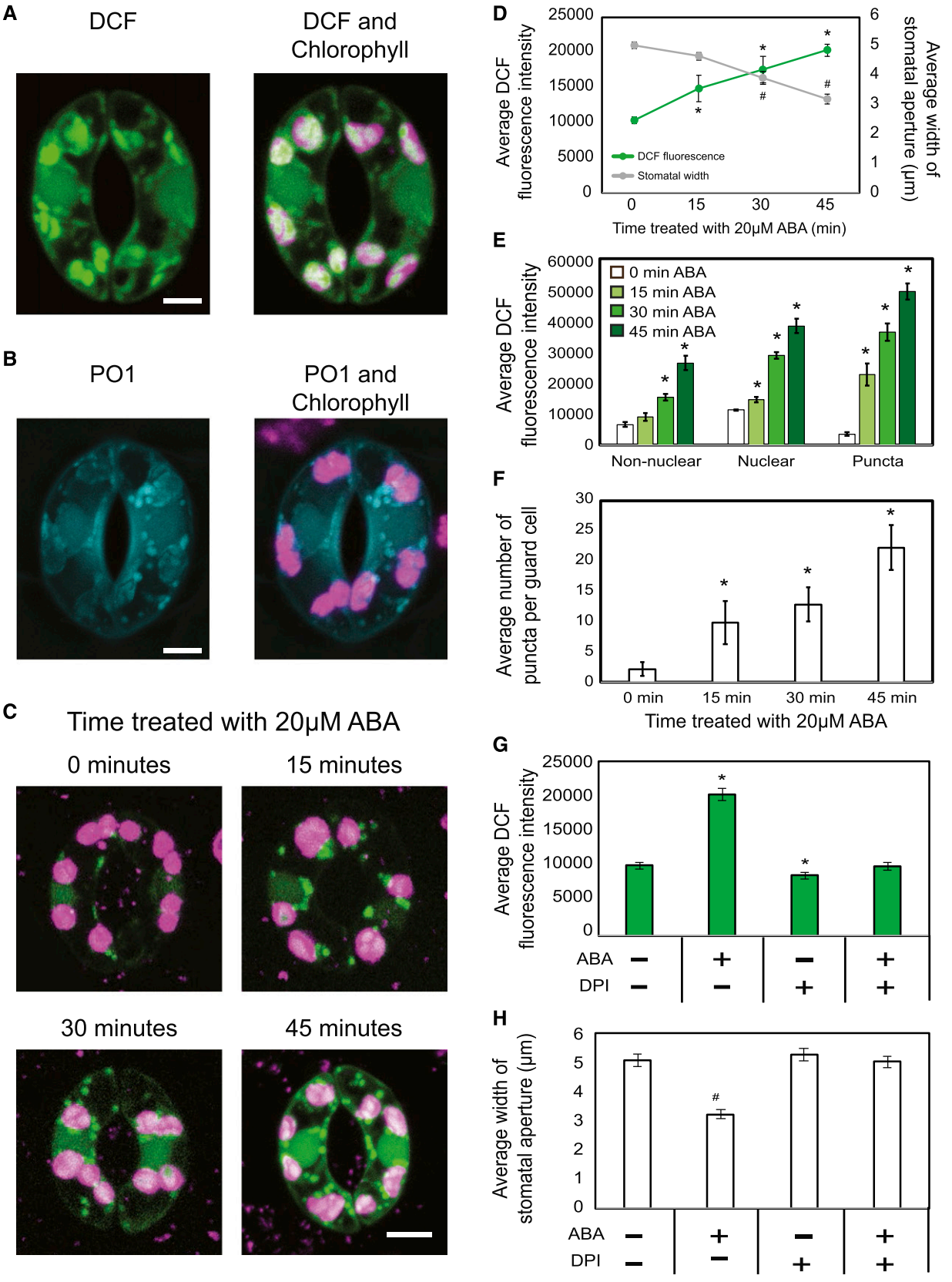

Figure 2. ABA-induced ROS burst in guard cells precedes stomatal closure in wild-type tomato leaves. A, Confocal micrographs of DCF fluorescence guard cells, with DCF signal in green and chlorophyll autofluorescence in magenta. B, Confocal

the punctate structures. DCF fluorescence increased steadily in the nuclei and in nonnuclear regions at each time point after ABA treatment, with 2.9- and 4.3-fold increases in DCF fluorescence between 0 and 45 min of ABA treatment, respectively (Fig. 2E). The greatest magnitude increase in DCF fluorescence was observed in the punctate structures, which showed a 13.6-fold increase after 45 min of ABA treatment. The signal in these structures also increased more rapidly, with a 6.6-fold increase at 15 min after treatment. Additionally, we observed an increase in the number of these DCF puncta in response to ABA, with a greater than 10.1-fold increase within 15 min after ABA treatment (Fig. 2F).

To determine if the ABA-induced ROS burst precedes ABA-dependent stomatal closure, we measured stomatal apertures at the same time points. After each treatment, epidermal peels were generated, stained with Toluidine Blue O, and imaged with bright-field microscopy. The aperture widths of at least 70 stomata at each time point over two separate experiments were quantified (Fig. 2D). We observed no significant difference in stomatal apertures after 15 min of ABA treatment; however, 30 and 45 min of ABA treatment resulted in significant decreases in stomatal aperture to 74% and 63% relative to time 0, respectively. No significant change was observed after 45 min of mock treatment, where stomatal aperture was 5.1 μm as compared with 5.2 μm for time 0 and 45 min, respectively.

To directly test whether RBOH-produced ROS drives stomatal closure, we blocked RBOH activity with the inhibitor diphenyleneiodonium chloride (DPI; Osaki et al., 2011), which reduces ROS levels and guard cell closure in Arabidopsis (Alvarez et al., 1998; Pei et al., 2000; Singh et al., 2017). Excised leaves were placed in stomatal opening solution with and without 100 μM DPI under white light for 3 h, with samples imaged directly or after the addition of ABA for 45 min. DPI treatment prevented the ROS burst after ABA treatment and led to slight, but significant, decreases in DCF signal in resting guard cells compared with the absence of DPI (Fig. 2G). Consistent with DCF-reported ROS changes, ABA-induced stomatal closure also was blocked by treatment with DPI, while it had no effect on fully open guard cells in the absence of ABA treatment (Fig. 2H). Together, these findings suggest that, in tomato, ABA-induced ROS bursts in guard cells precede and are required for ABA-induced stomatal closure.

Flavonols Accumulate in Guard Cells, with Altered Levels in Tomato Anthocyanin Mutants

To ask if flavonols accumulate in guard cells of tomato leaves, we used diphenylboric acid 2-aminoethyl ester (DPBA). DPBA is a fluorescent dye that binds to kaempferol and quercetin and their glycosides in the wild type but shows no signal in flavonol-deficient mutants (Lewis et al., 2011). DPBA has been used to image flavonol accumulation in roots and guard cells of Arabidopsis (Brown et al., 2001; Peer et al., 2001; Lewis et al., 2011; Watkins et al., 2014). Confocal images generated using spectral imaging of the basal surface of whole tomato leaves show DPBA fluorescence in the yellow channel and chlorophyll autofluorescence in the magenta channel. Flavonol accumulation is present in guard cells but not in the surrounding pavement cells, consistent with guard cell-specific accumulation of flavonols (Fig. 3A). DPBA fluorescence appeared brightest in a region that was of the position and size of a guard cell nucleus. The fluorescence of DPBA and Hoechst, a nucleic acid stain, in the same guard cells overlaps, consistent with the nuclear accumulation of flavonols (Supplemental Fig. S1). DPBA fluorescence also is observed in nonnuclear regions of guard cells. To ask if this accumulation is in the vacuole or cytoplasm, we used the vacuole dye Acridine Orange, as shown in Supplemental Figure S3. Unfortunately, DPBA and this dye were not chemically and optically compatible, so they had to be imaged in separate guard cells. These images suggest that DPBA is found in both the cytoplasm and vacuole, but parallel imaging cannot make this point conclusively.

We examined two tomato mutants with altered accumulation of anthocyanins, which are products of the flavonoid pathway. The mutant *are* has a defect in the gene encoding F3H (Fig. 1), resulting in reduced flavonols in the hypocotyls and roots of young seedlings (Yoder et al., 1994; Maloney et al., 2014). The mutant *aw* has a defect in the gene encoding DFR, which uses dihydroflavonols as substrates in the first step of anthocyanin biosynthesis, so the defect in this enzyme results in increased levels of flavonols and the absence

Figure 2. (*Continued.*)
micrographs of PO1 fluorescence in guard cells, with PO1 signal in blue and chlorophyll autofluorescence in magenta. C, Increases in DCF fluorescence visualized in guard cells across a 45-min time course of ABA treatment in the Ailsa Craig (AC) genotype. D, DCF fluorescence in entire guard cells and stomatal aperture shown as a function of time after treatment with 20 μM ABA. Asterisks and number signs represent significant differences in DCF fluorescence ($P < 0.001$) and stomatal aperture ($P < 0.009$) between time 0 and the indicated times or between untreated and treated, respectively. E, DCF signal was quantified in specific regions separately as a function of time after ABA treatment in 30 guard cells. Asterisks represent significant differences in DCF fluorescence ($P < 0.001$) between time points within a cellular location. F, The number of puncta was quantified as time after ABA treatment in 30 guard cells. Asterisks represent significant differences in the number of puncta per guard cell ($P < 0.01$) between time points. G and H, DCF fluorescence (G) and stomatal aperture (H) were quantified with and without 100 μM DPI at 0 and 45 min of treatment with ABA. Asterisks and number signs represent significant differences in DCF fluorescence ($P < 0.001$) and stomatal aperture ($P < 0.001$) between time 0 and the indicated times or between untreated and treated, respectively. Statistics were determined using two-way ANOVA followed by Tukey's posthoc test. $n = 70$. Bars = 5 μm.

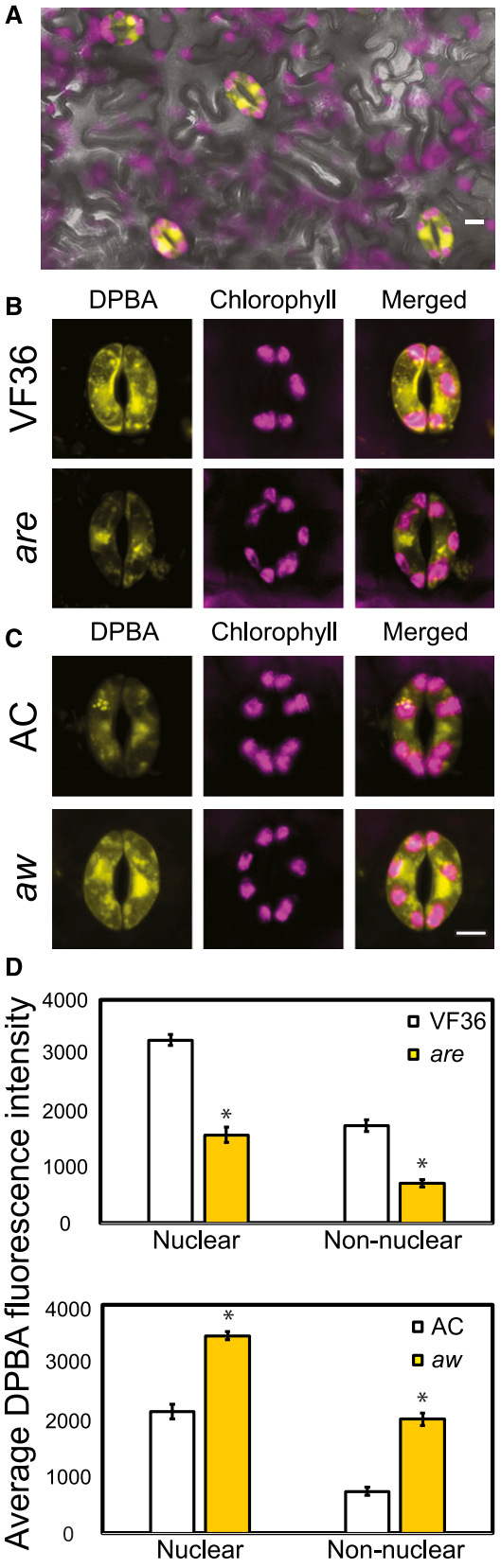

Figure 3. Tomato anthocyanin mutants have altered levels of flavonol accumulation in guard cells. Confocal micrographs show DPBA-bound flavonols in yellow and chlorophyll autofluorescence in magenta. A, DPBA fluorescence was visualized in a whole leaf. B and C, DPBA fluorescence and chlorophyll autofluorescence were examined in tomato guard cells in *are* and *aw* mutant guard cells and their wild-type parental lines, VF36 and AC, respectively. D, Quantifications of relative DPBA fluorescence in 90 samples from three separate experiments. Asterisks represent significant differences ($P < 0.001$) between the mutant and the wild type within a cellular location. Statistics were determined using two-way ANOVA followed by Tukey's posthoc test. $n = 90$. Bars = 5 μm.

of anthocyanins (Goldsbrough et al., 1994; Ballester et al., 2010; Maloney et al., 2014). DPBA fluorescence was examined by LSCM, and representative images are shown in Figure 3, B and C. We quantified fluorescence in 90 guard cells over three separate experiments. Flavonol accumulation in the nucleus and a nonnuclear region of *are* guard cells was at 52% and 59% of the levels in the parental line, VF36, respectively (Fig. 3D). Flavonol accumulation was 1.5- and 1.8-fold higher in the nucleus and nonnuclear regions of *aw* mutant guard cells than VF36, respectively. The flavonol levels in the two wild types cannot be compared directly, nor can the magnitude of the difference in the mutants relative to their wild-type parents, as we optimized confocal images for each panel separately to obtain maximal signal for comparison of the mutants with their parental lines.

We employed high-pressure liquid chromatography-mass spectroscopy (LC-MS) to quantify concentrations of flavonols in fully expanded leaves to demonstrate that DPBA fluorescence accurately reported changes in the abundance of flavonols in the *are* and *aw* mutants grown under these conditions. Hydrolyzed flavonol samples were extracted from 27 fully expanded leaves of 5-week-old VF36, *are*, AC, and *aw* plants and analyzed to examine the total pools of naringenin, a flavonol precursor, and the flavonols kaempferol and quercetin (Table I). Naringenin levels in *are* were significantly higher than in the wild type due to the mutation in the *F3H* gene in *are*, while kaempferol and quercetin were significantly lower in *are* compared with the wild type. The *aw* mutant had 3.1- and 1.4-fold higher levels of naringenin and quercetin, respectively, with a significant 7.6-fold increase in kaempferol. These measurements show similar trends to the localized accumulation of flavonols, as judged by DPBA fluorescence intensities, in the guard cells of each mutant.

Flavonol Accumulation in Guard Cells Modulates ROS Homeostasis

We observed steady-state ROS levels in guard cells of tomato flavonoid mutants *are* and *aw* by imaging DCF fluorescence to ask if altered flavonol levels in these guard cells would modulate ROS. Epidermal peels were generated from freshly excised leaves and stained with CM H_2DCF-DA. Confocal micrographs of leaf peels of the basal surface of tomato leaves show DCF fluorescence present in the nucleus and nonnuclear area of guard cells, with higher levels of DCF fluorescence

Table I. *Quantification of flavonoids from fully expanded leaves from 4- to 5-week-old tomato plants*

Quantification of flavonoids is shown from fully expanded leaf tissue by LC-MS. Average values ± SE are presented in pmol g^{-1} fresh weight. Samples were analyzed from three different biological replicates using three technical replicates on three different occasions, resulting in $n = 18$ for naringenin in VF36 and $n = 27$ for naringenin for *are*; kaempferol and quercetin have $n = 27$ for the wild type and *are*. Naringenin has $n = 12$ for AC and $n = 16$ for *aw*; kaempferol and quercetin have $n = 24$ for the wild type and *aw*. Asterisks indicate significant differences from the wild type as indicated by Student's *t* test (***$P < 0.001$, **$P < 0.01$, and *$P < 0.05$).

Flavonoid	VF36	*are*	Ratio[a]	AC	*aw*	Ratio[b]
Naringenin	0.70 ± 0.16	11.4 ± 1.5 ***	16.3 ± 2.1	2.37 ± 0.76	7.29 ± 1.20	3.1 ± 0.5
Kaempferol	3,812 ± 515	118.0 ± 7.2***	0.03 ± 0.002	1,567 ± 348	11,912 ± 1,332**	7.6 ± 0.9
Quercetin	54,931 ± 7,209	20,383 ± 2,371*	0.37 ± 0.04	59,005 ± 8,109	84,264 ± 7,512	1.4 ± 0.1

[a]Ratio represents the mutant *are* values divided by the wild-type values. [b]Ratio represents the mutant *aw* values divided by the wild-type values.

found in nuclei (Fig. 4, A and B). ROS accumulation was inversely proportional to flavonol accumulation in *are* and *aw*. The nonnuclear area of *are* guard cells had a 1.5-fold higher level of DCF fluorescence than the wild type. The *aw* mutant had DCF fluorescence levels that were 58% of its parental genotype (Fig. 4C). Together, these results demonstrate that flavonol concentrations are inversely proportional to ROS levels across these four genotypes, suggesting that flavonols act as antioxidants in tomato guard cells.

We also quantified subcellular steady-state H_2O_2 levels in VF36 and *are* using PO1, a fluorescent sensor used for imaging H_2O_2 (Fig. 5). PO1 fluorescence quantified from whole guard cells was 1.7-fold greater in *are* compared with VF36 (Fig. 5B). PO1 fluorescence was observed in punctate structures that resembled endomembranes and associated with chloroplasts, similar to the fluorescence pattern observed with DCF staining. PO1 fluorescence was greater in each subcellular location in *are* compared with VF36, with 1.4-, 2-, and 1.9-fold increases in nuclear, nonnuclear, and punctate structures, respectively (Fig. 5C). Additionally, we observed a 5.9-fold increase in the number of these PO1 puncta in *are* (Fig. 5D).

Flavonols in Guard Cells Modulate ABA-Induced Changes in ROS and Stomatal Closure

The effect of altered accumulation of flavonol antioxidants on the kinetics of ABA-induced DCF accumulation and stomatal closure was examined in the flavonoid mutants. Whole leaves of *are* and *aw* and their respective backgrounds were excised and incubated in stomatal opening buffer for 3 h under white light followed by treatment with 20 μM ABA for 0, 15, 30, and 45 min. After each treatment, epidermal peels were generated and stained with CM H_2DCF-DA (Fig. 6, A and B). Confocal micrographs show no significant differences in DCF fluorescence levels in any genotype after 0 min of ABA treatment due to the incubation in stomatal opening buffer. After treatment with ABA, increases in DCF fluorescence were observed in wild-type and mutant guard cells, with levels inversely proportional to flavonol levels (Fig. 6, A and B). Quantification of DCF fluorescence (in at least 30 guard cells) increased across the 45-min time course of ABA treatment as determined by two-way ANOVA followed by Tukey's posthoc test. The slope of the entire time course is more than 2-fold greater in *are* than in VF36 ($R^2 > 0.98$), while the slope of AC is 1.8-fold faster than in *aw* ($R^2 > 0.97$; Fig. 6B). As the DCF fluorescence change is most rapid between 0 and 15 min, we also examined the initial velocities of these lines. The initial velocities were higher in *are* compared with VF36, showing a 2.5-fold increase in slope. Additionally, the initial rate of DCF fluorescence increase was significantly slower in *aw*, with a slope that is 38.6% slower than that in AC.

To analyze the effects of ABA-induced ROS accumulation on stomatal closure, we excised whole leaves of *are* and *aw* and their respective parental lines and performed an identical ABA time course. The aperture widths of at least 90 stomata at each time point for two separate experiments were quantified. Stomata from untreated leaves showed an average opening of 5 μm for both the wild type and mutants (Fig. 6C). In the guard cells of *are* leaves, which have a lower concentration of flavonols and more ROS, we observed a 1.5-fold greater rate of stomatal closure in *are* in response to ABA treatment over the entire time course compared with the wild type, with a 3-fold increase in initial velocities in *are* as compared with VF36. In guard cells of *aw* leaves, which have greater flavonol levels and less ROS, we observed a significant reduction in slope, with 1.5-fold greater ABA response in AC than in *aw* (Fig. 6D). Initial velocities showed a 2.7-fold increase in AC and *aw*. The stomata of *aw* did not show a significant difference in closure until 30 min of ABA compared with time 0, which is consistent with DCF fluorescence intensities in *aw* in response to ABA (Fig. 6F). These results reinforce the model that ROS bursts precede ABA-induced stomatal closure and illustrate the inverse relationship between the levels of flavonols and ROS that we observed in *are* and *aw*, which are linked to altered rates of ABA-dependent stomatal closure.

Guard Cell-Localized Flavonol Accumulation Facilitates Stomatal Opening in Response to Light

Stomatal aperture also was examined in the flavonoid mutants to determine how flavonols impact the guard cell response to light-dependent opening. Excised leaves of *are* and *aw* and their respective parental

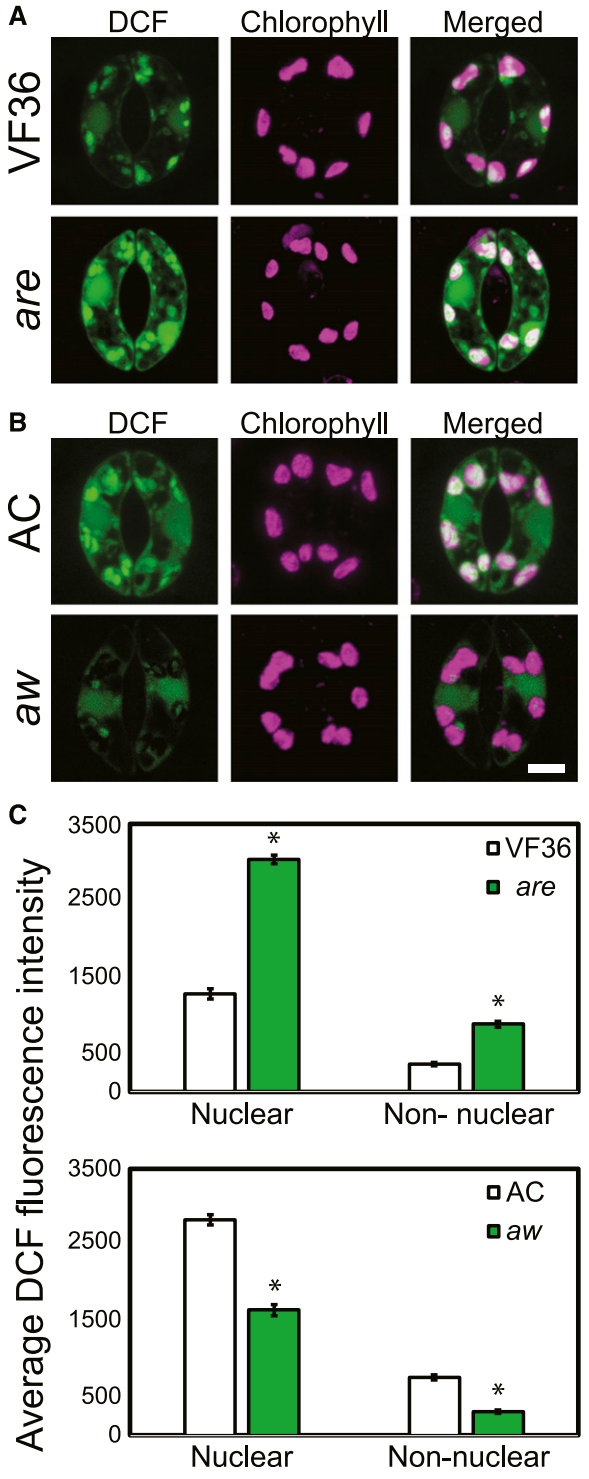

Figure 4. The levels of DCF fluorescence in guard cells are inversely related to the levels of flavonols. A and B, Confocal micrographs showing DCF fluorescence in *are* and *aw* and their parental lines. C, Quantification of relative DCF fluorescence in 90 samples over three separate experiments, with averages ± SE reported. Asterisks represent significant differences ($P < 0.001$) between the mutant and the wild type within a cellular location. Statistics were determined using two-way ANOVA followed by Tukey's posthoc test. Bar = 5 μm.

lines were incubated in the dark in the presence of 20 μM ABA for 3 h to fully close stomata before being transferred to stomatal opening buffer without ABA in the light for 45 min. The aperture widths of at least 30 stomata at each time point for three separate experiments were quantified. Stomata from dark-adapted leaves showed an average opening of 1 μm for both the wild type and mutants (Fig. 7A). In the guard cells of *are* leaves, which have a lower concentration of flavonols and more ROS, we observed reduced stomatal opening in response to light compared with the wild type, with average aperture values of 2.5 and 3.9 μm for mutant and parental lines, respectively. In guard cells of *aw* leaves, which have greater flavonol levels and less ROS, we observed a significant difference between genotypes, with more stomatal opening in response to light in *aw* compared with the wild type, with apertures of 3.9 and 4.8 μm, respectively (Fig. 7A). These results are consistent with flavonols functioning to minimize ROS, which then allows light-induced stomatal opening to occur more rapidly. Mutants with reduced flavonols maintain the closed state for longer periods of time.

To determine if there are decreases in ROS that allow light-induced guard cell opening, the levels of DCF were examined in these genotypes using the same time line of treatment. DCF fluorescence after 3 h in the dark in ABA was similar in the wild type and *are* but was reduced in *aw*, consistent with higher antioxidant levels. DCF signal decreased in each genotype after light treatment (Fig. 7B). In the wild types, DCF decreased to 78% or 76% of starting levels upon transfer to the light for VF36 or AC, respectively. The magnitude decrease was enhanced in the flavonol-elevated mutant *aw* to 61% of the starting value and decreased in the flavonol-reduced mutant *are* to 92% of its starting value (Fig. 7C). These results indicate an important role of flavonols in dampening ROS to allow light-dependent guard cell opening.

Excised Leaves of Tomato Anthocyanin Mutants Show Altered Rates of Water Loss That Correspond to Stomatal Aperture

If flavonols in guard cells function to inhibit ABA-induced stomatal closure by scavenging ROS, then lower rates of transpiration would be predicted in *are* leaves that have less flavonols and higher rates would be predicted in *aw* leaves that have more flavonols (Fig. 8). To assess the effects of flavonol levels in guard cells on transpiration, we monitored water loss from excised leaves over a 40-min time course. Leaves of flavonol-reduced *are* exhibited reduced water loss and leaves of flavonol-elevated *aw* exhibited enhanced water loss compared with the parental lines (Fig. 8A), as determined by two-way ANOVA. This finding is consistent with flavonol accumulation in guard cells modulating stomatal aperture, thereby modulating transpiration rates. Significant differences in water loss between

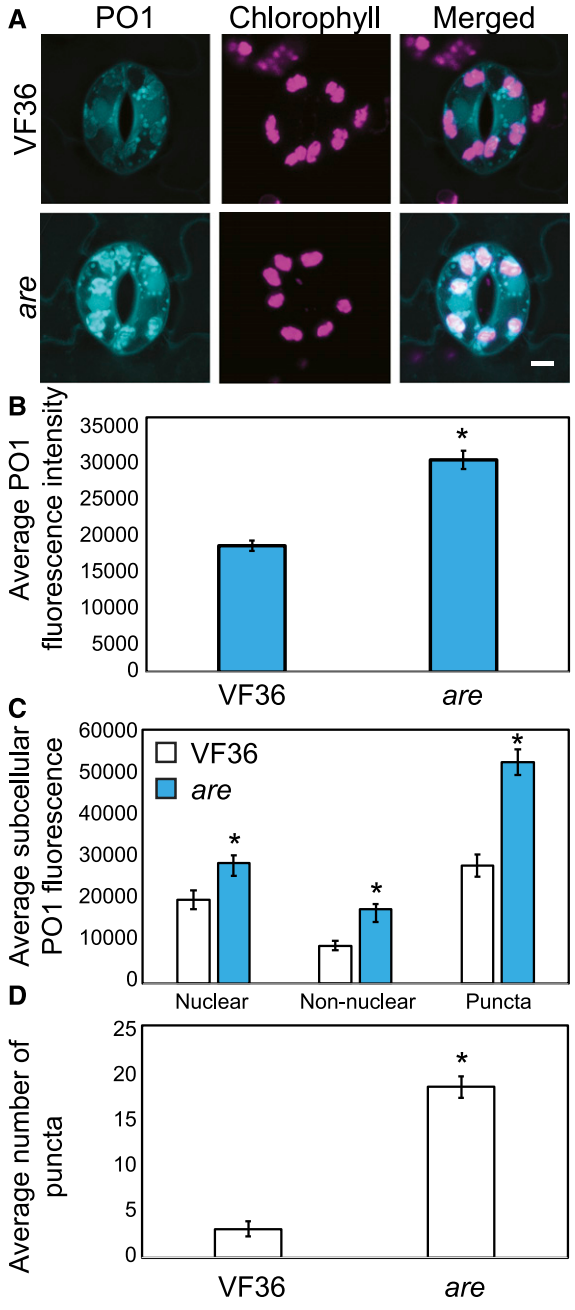

Figure 5. The levels of PO1 fluorescence in guard cells are higher in *are* compared with VF36. A, Confocal micrographs showing PO1 fluorescence in VF36 and *are*. B, Quantification of relative PO1 fluorescence in 30 samples over two separate experiments, with averages ± SE reported. The asterisk represents a significant difference ($P < 0.001$) between the mutant and the wild type. C, The PO1 signal was quantified in specific regions in VF36 and *are* in 30 guard cells. Asterisks represent significant differences in DCF fluorescence ($P < 0.001$) between genotypes within a cellular location. D, The number of puncta was quantified in VF36 and *are* in 30 guard cells. The asterisk represents a significant difference in the number of puncta per guard cell ($P < 0.01$) between genotypes. Statistics were determined using two-way ANOVA followed by Tukey's posthoc test. Bar = 5 μm.

tomato plants in the VF36 background and the AC background also were observed.

Differences in water loss between flavonol mutants could be due to altered guard cell aperture, different stomatal density, or larger stomatal size. To separate these three possibilities, stomatal densities (number of stomata per 1.5 mm^2) were determined using epidermal peels from fully expanded leaves. Quantification of stomatal densities from three leaves from separate plants revealed that stomata are found at greater density on average in VF36 than in AC, which could explain the enhanced water loss measured in VF36 relative to AC (Fig. 8, B and C). There were no differences between VF36 and *are* or between AC and *aw*, which is consistent with aperture, rather than stomatal density, causing altered water loss in the mutants. To verify that the mutations did not affect the overall size of stomata, we compared the lengths of stomata from wild-type and mutant leaves. The length of stomatal pores was not significantly different between *are* (10.8 ± 0.3 μm) and its parental line, VF36 (10.5 ± 0.2 μm), or between *aw* (14.2 ± 0.3 μm) and its parental line, AC (13.9 ± 0.3 μm). Together, these results show that enhanced water loss in *are* and reduced water loss in *aw* leaves are consistent with differences in flavonol levels in guard cells and are not tied to differences in leaf anatomy or guard cell development.

Ethylene Induces Flavonol Accumulation, Decreases ROS, and Inhibits Stomatal Closure

The flavonoid biosynthetic pathway is highly regulated, which may be one mechanism by which guard cell signaling is modulated to respond to environmental changes. Elevated ethylene enhances flavonol accumulation in Arabidopsis roots and guard cells (Lewis et al., 2011; Watkins et al., 2014), so we asked whether exogenous ethylene treatment would induce flavonol accumulation in tomato guard cells. We treated intact Pearson wild-type and *Nr* tomato plants, which has a gain-of-function mutation in the ethylene receptor, yielding ethylene-insensitive plants (Yen et al., 1995), with and without 5 μL L^{-1} ethylene gas for 24 h. We then imaged DPBA fluorescence in 30 stomata per treatment for three separate experiments. In the absence of exogenous ethylene, guard cells of *Nr* plants exhibited a slightly lower, but not significant, difference in DPBA fluorescence relative to Pearson. In the presence of ethylene, there was a significant 1.4-fold increase in DPBA fluorescence in Pearson, but in *Nr*, there was no increase in DPBA fluorescence after ethylene treatment (Fig. 9).

The levels of ROS also were examined in guard cells of Pearson and *Nr* plants with and without ethylene treatment. After exogenous ethylene treatment of whole plants, leaf peels of Pearson and *Nr* were stained with CM H_2DCF-DA, and DCF fluorescence was quantified using LSCM. We observed 1.3-fold more DCF fluorescence in untreated *Nr* guard cells compared with Pearson (Fig. 9). Ethylene treatment of Pearson guard cells exhibited 47%

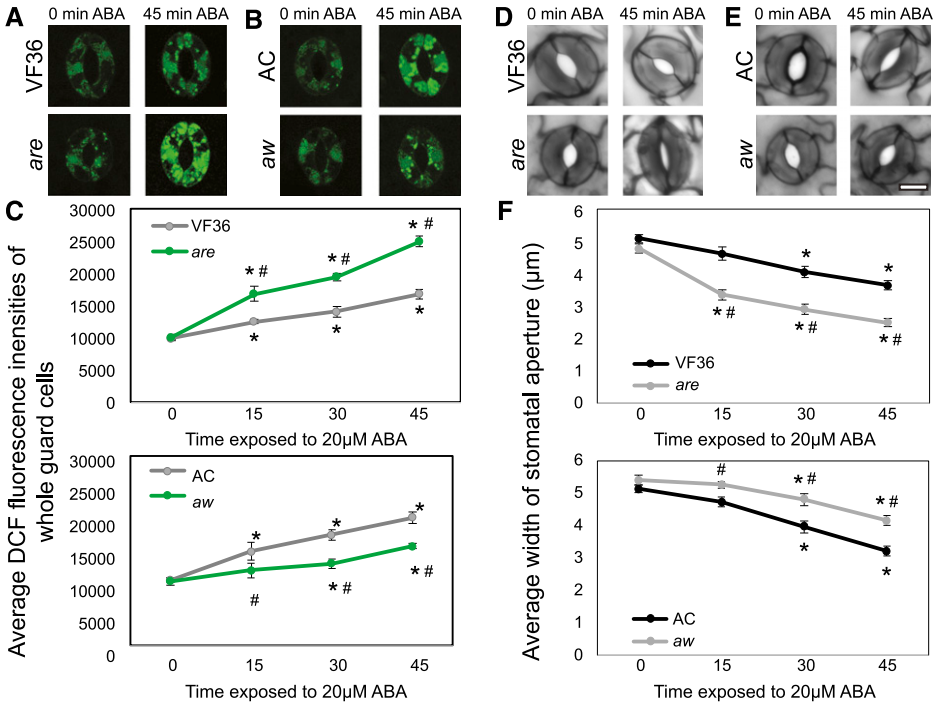

Figure 6. Flavonols alter ABA-induced changes in ROS and guard cell closure. A and B, Confocal micrographs of DCF fluorescence (green) in *are* and *aw* and their corresponding backgrounds are shown in the absence and presence of 20 μM ABA solution for 0, 15, 30, and 45 min. C, DCF fluorescence was quantified at the indicated times after ABA treatment. Averages ± SE of 40 guard cells per genotype per treatment time are reported. D and E, Stomatal apertures of leaves of *are* and *aw* and their corresponding backgrounds are shown in the absence and presence of ABA for 45 min. F, The aperture of mutants was measured after ABA treatment at each time point listed above. Averages ± SE of 90 stomata for each genotype and time point from two separate experiments are reported. For all graphs, asterisks and number signs represent significant differences ($P < 0.001$) between time treated with ABA and time 0 or between mutant and wild type within the same time point, respectively, using two-way ANOVA followed by Tukey's post hoc test. Bar = 5 μm.

of the DCF fluorescence as compared with untreated controls, consistent with elevated flavonol antioxidants in the presence of ethylene. In contrast, DCF fluorescence in *Nr* guard cells did not change significantly in response to ethylene treatment. Together, these results are consistent with ethylene reducing ROS concentrations in guard cells by inducing the synthesis of flavonol antioxidants.

To analyze the effect of ethylene-induced flavonols in tomato guard cells, we observed ABA-induced stomatal closure in Pearson and *Nr* with and without ethylene treatment. Intact leaves from Pearson and *Nr* with and without 24 h of ethylene treatment were excised and incubated in stomatal opening buffer for 3 h followed by treatment with 20 μM ABA for 0 or 45 min. The aperture widths of at least 30 stomata at each time point for three separate experiments were quantified using ImageJ. Stomata from untreated leaves showed an average opening of 6 μm for both Pearson and *Nr* (Fig. 9). The apertures of Pearson stomata in the absence of ethylene were reduced to 48% of the untreated control by ABA. Ethylene-treated Pearson, with elevated flavonols, was less responsive to ABA, which only closed to 20% of untreated values. *Nr* stomata showed a greater closure, consistent with reduced flavonols and greater ROS, with 66% and 64% stomatal closure in untreated and ethylene-treated plants, respectively, in response to ABA treatment. These genotypes have equivalent stomatal sizes, with Pearson and *Nr* stomata being, on average, 14.5 ± 0.3 and 14.8 ± 0.3 μm long, respectively. The differences in stomatal apertures in response to ABA are consistent with ethylene-induced flavonols reducing ROS in the wild type, but not *Nr*, and thereby reducing the rate of the stomatal closure pathway.

To ask if the effects of ethylene on stomatal aperture are linked directly to flavonol accumulation in guard cells, we examined the effects of ethylene treatment on flavonol levels and ABA-induced stomatal closure in VF36 and *are* (Fig. 10). DPBA imaging of guard cells was performed on VF36 and *are* leaves treated with and without 5 μL L^{-1} ethylene gas for 24 h. Similar to our previous results, we observed greater DPBA fluorescence in guard cells of VF36 compared with *are*, with 1.8-fold higher levels in VF36 in the absence of ethylene (Fig. 10A). In the presence of ethylene, there was a significant 1.6-fold increase in DPBA fluorescence in VF36 and a 1.5-fold increase in *are*. This yields a 1.9-fold change in DPBA signal between VF36 and *are* after ethylene treatment. We asked whether the effect of ethylene on guard cell closure also was attenuated in the *are* mutant.

To ask whether the ethylene modulation of the guard cell aperture acts through flavonols, we compared ethylene and

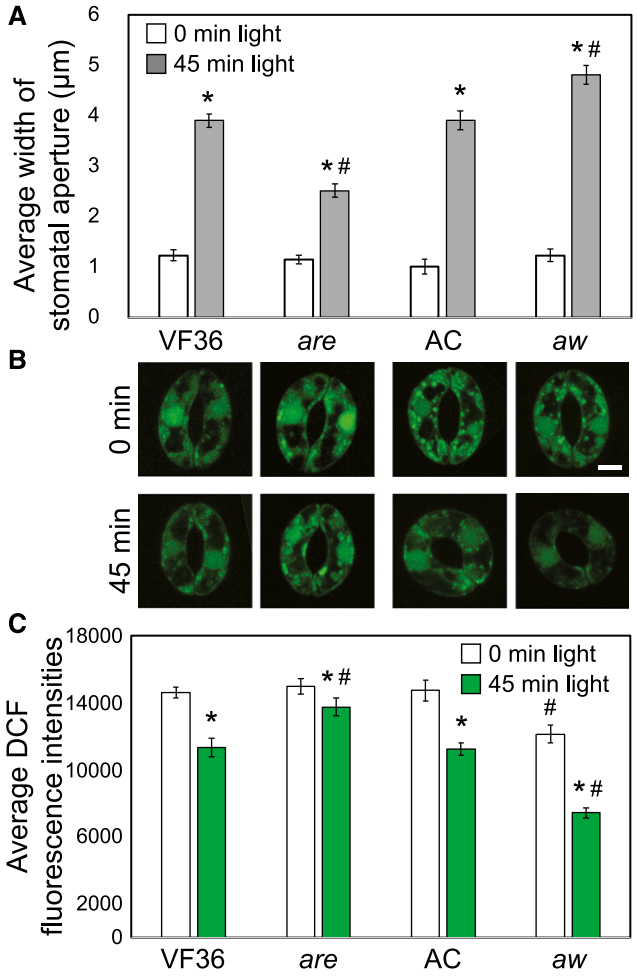

Figure 7. Flavonoid mutants have altered stomatal opening in response to light. A, Excised leaves of *are* and *aw* and their respective parental lines were incubated in the dark in the presence of 20 μM ABA for 3 h before being transferred to stomatal opening buffer without ABA in the light for 45 min. Averages ± SE of 90 stomata from three separate experiments are reported. B, Confocal micrographs of DCF fluorescence (green) in *are* and *aw* and their corresponding backgrounds are shown before and after treatment with light. C, DCF fluorescence was quantified before and after light treatment. Averages ± SE of 50 samples across two experimental replicates are reported. Asterisks and number signs represent significant differences ($P < 0.001$) between time exposed to light and time 0 and between mutant and wild type within the same time point, respectively, determined using two-way ANOVA followed by Tukey's post hoc test. Bar = 5 μm.

ABA responses in VF36 and *are*. ABA reduced the aperture of VF36 stomata in the absence of ethylene to 78% of the untreated control, while, in the presence of ethylene, ABA treatment only reduced closure to 86% of untreated values (Fig. 10B). The effect of ABA on untreated *are* guard cell closure was greater than in VF36, closing to 61% of untreated values. Consistent with the hypothesis that ethylene mediates its effect on closure through flavonols, we observed less response to ABA in *are* treated with ethylene, with 74% stomatal closure in the presence of ethylene (as compared with 86% in VF36). The increase in DPBA fluorescence in *are* treated with ethylene likely explains the ethylene effect on stomatal closure in this mutant. The differences in ABA-induced stomatal closure and DPBA fluorescence in response to ethylene are consistent with ethylene modulating stomatal closure by inducing flavonol accumulation in guard cells.

DISCUSSION

ROS signaling has been studied in Arabidopsis, but less is known about the signaling roles of ROS in agricultural species. In Arabidopsis guard cells, the hormone ABA positively regulates RBOH enzyme activity. Activated RBOHs rapidly synthesize ROS, which act as second messengers to induce stomatal closure (Mittler and Blumwald, 2015; Balmant et al., 2016; Sierla et al., 2016). To prevent oxidative damage, ROS signaling must be tightly regulated by small molecule and/or protein antioxidants so that ROS elevation is transient and rapidly returns to nondamaging levels, restoring ROS homeostasis (Conklin et al., 1996; Apel and Hirt, 2004; Gayomba et al., 2017). Even less is known about the function of these antioxidants in crop species, such as tomato, which are grown in much harsher environmental conditions than Arabidopsis. The elevated light and temperature under standard field conditions may increase antioxidant stress and flavonol levels. In this study, we asked if tomato uses an RBOH-induced ROS burst to close stomata and whether flavonol antioxidants modulate ROS levels and ABA-dependent guard cell closure, light-dependent guard cell opening, and whole leaf physiology.

A critical first step in these experiments was to ask whether a ROS burst drives stomatal closure in tomato guard cells. We examined ABA-induced ROS bursts and ABA-dependent stomatal closure in tomato guard cells over a 45-min time course. Fluorescence of the general ROS sensor, DCF, increased in guard cells, with significant changes preceding the induction of stomatal closure (Fig. 2). To ask if ABA leads to increases in ROS by the activation of an RBOH enzyme, we used DPI to inhibit RBOH. DPI blocked both ABA-induced ROS production and stomatal closure in tomato guard cells. These results are consistent with ABA signaling in tomato inducing RBOH to produce ROS and close stomata.

Imaging of ROS levels using DCF, a general ROS sensor, and PO1, an H_2O_2 selective reporter, on a new confocal microscope provides significant new insight into where these molecules accumulate. DCF and PO1 signals accumulate in the nucleus, as demonstrated by DCF colocalization with Hoechst stain, where ROS plays a role by changing the activity of redox-sensitive transcription factors (Willems et al., 2016). DCF signal has been observed previously in the guard cell cytoplasm (Lee et al., 1999; Kwak et al., 2003; Chen and Gallie, 2004; Watkins et al., 2014; Xia et al., 2014; An et al., 2016), but the images within this data set use an

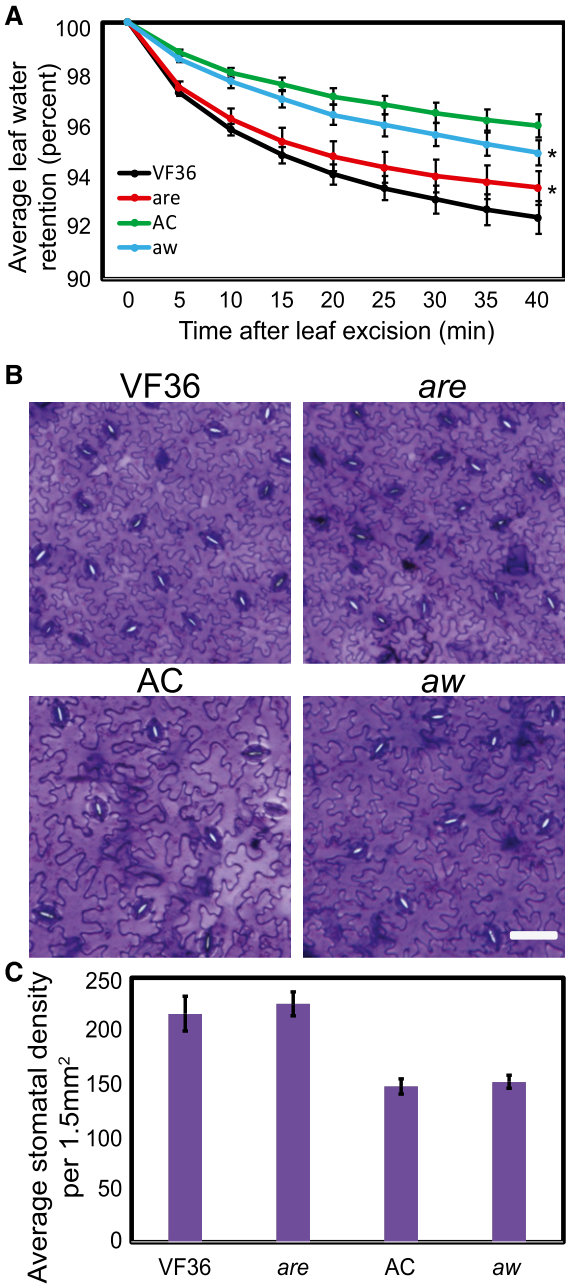

Figure 8. Flavonoid mutants have altered water loss from excised tomato leaves and stomatal responses to light. A, Fully expanded leaves were excised from well-watered plants in the afternoon and immediately weighed at 5-min intervals. Four leaves from four different plants were used in four separate experiments ($n = 16$). Asterisks represent significant differences ($P < 0.005$) between the mutant and the wild-type time course, determined using two-way ANOVA. B, Bright-field images of wild-type and mutant epidermal peels stained with Toluidine Blue 0. C, Quantification of stomatal density in wild-type and mutant leaves. Stomatal density was quantified from three fully expanded leaves from separate plants. Statistics were determined using two-way ANOVA followed by Tukey's posthoc test comparing genotype by time ($P < 0.005$). Bar = 30 μm.

LSCM device with greater sensitivity to show complex subcellular localization patterns of DCF and PO1 fluorescence in guard cells. DCF and PO1 signal were found internal to chloroplasts and in small pockets next to chloroplasts (Supplemental Fig. S2), which also produce ROS as a product of various metabolic pathways (Suzuki et al., 2012).

DCF and PO1 fluorescence also accumulated in punctate regions resembling ROS-producing peroxisomal or endosomal organelles (Leshem et al., 2007; Sandalio and Romero-Puertas, 2015) and that are reminiscent of ROS synthesis by RBOH enzymes embedded in membranes of mammalian redoxosomes (Brown and Griendling, 2009). The detection of these signals with PO1, which is a boronate-based fluorescent probe that is selective for H_2O_2 (Lin et al., 2013; Liang et al., 2014), also is consistent with RBOH-induced elevation of H_2O_2. The similar accumulation of these two sensors in distinct spatial localizations is consistent with localized ROS accumulation, but like all experiments with exogenously added sensors, we cannot eliminate the possibility that there are localized accumulation patterns due to dye partitioning.

RBOH-induced ROS bursts are well studied in Arabidopsis due to the presence of null mutants in RBOH genes (Foreman et al., 2003; Kwak et al., 2003; Müller et al., 2009; Li et al., 2015; Orman-Ligeza et al., 2016; Choudhury et al., 2017). Isoforms AtRBOHF and AtRBOHD have been shown to be expressed in guard cells, where they function in the ABA-dependent stomatal closure pathway (Kwak et al., 2003). Like RBOH mutations, DPI has been shown to prevent ABA-induced ROS bursts, inhibiting stomatal closure in Arabidopsis (Pei et al., 2000; Suhita et al., 2004; Singh et al., 2017). Although tomato RBOH mutants are not available, *SIRBOH1*, a homolog of Arabidopsis *RBOHF*, has the target of virus-induced gene silencing to demonstrate that there is less CO_2- and salt stress-induced stomatal closure and that the response to ABA is reduced (Shi et al., 2015; Yi et al., 2015). Another study showed that brassinosteroid signaling functions through RBOH enzymes to induce stomatal closure (Xia et al., 2014). Together, these studies support the model that tomato guard cell closure requires an ABA-induced ROS burst, but what has not been examined in tomato is whether ROS homeostasis is regulated by antioxidants.

For flavonols to regulate ROS homeostasis in tomato guard cells, these antioxidants and their biosynthetic machinery must be localized to these cells and to subcellular locations where ROS accumulate. We examined flavonol accumulation and localization using a dye, DPBA, that binds specifically to kaempferol and quercetin and their glycosides (Buer and Muday, 2004; Lewis et al., 2011). DPBA fluorescence accumulates in guard cells, but not surrounding pavement cells, of wild-type tomato leaves (Fig. 3). The signal accumulates in the nucleus, consistent with prior reports (Saslowsky et al., 2005; Lewis et al., 2011; Watkins et al., 2014), where it may regulate redox-sensitive transcription factors and or prevent ROS-induced DNA damage. DPBA also may accumulate in both the cytoplasm

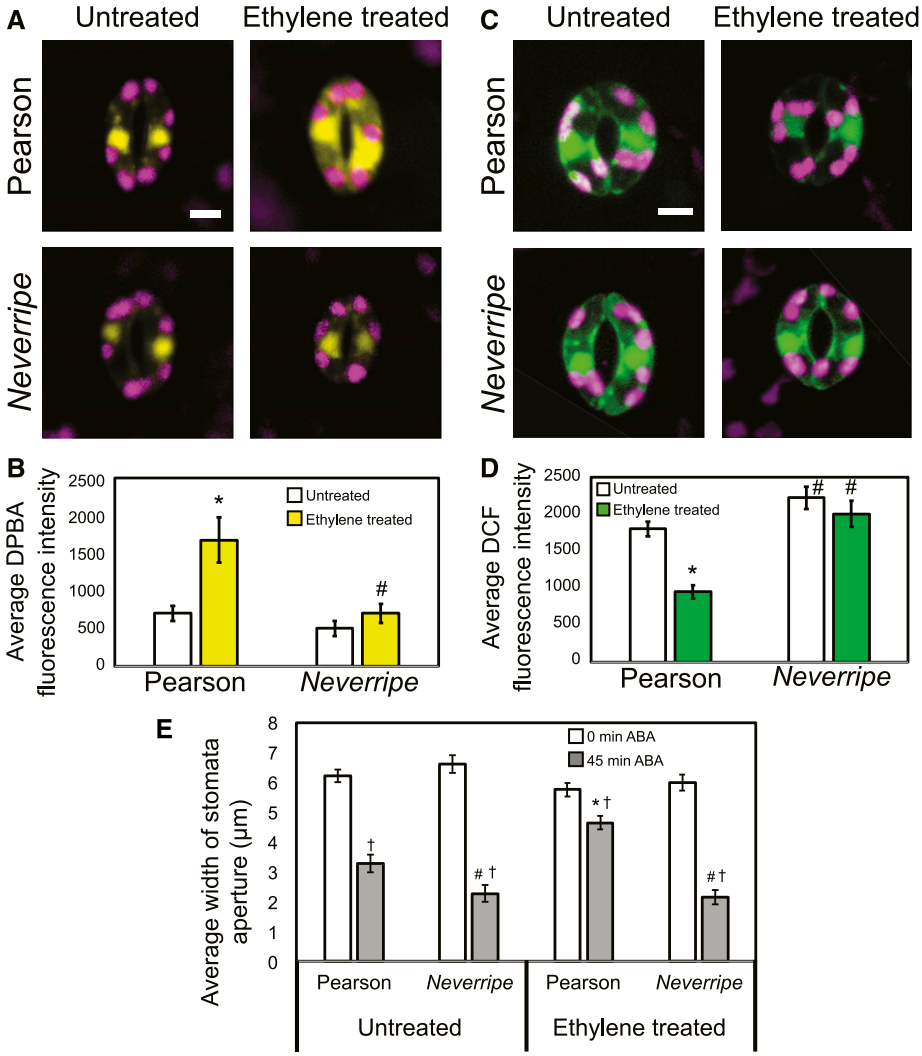

Figure 9. Ethylene treatment increases flavonol accumulation, decreases ROS accumulation, and reduces stomatal closure in guard cells of Pearson but not *Nr* plants. A, DPBA fluorescence in Pearson and *Nr* guard cells with and without treatment with 5 μL L^{-1} ethylene gas for 24 h visualized by LSCM. B, Averages ± SE of DPBA fluorescence in the cytosol of 90 guard cells are reported. C, Confocal micrographs showing ROS accumulation of Pearson and *Nr* guard cells with and without ethylene. D, Averages ± SE of DCF fluorescence in the cytosol of 90 guard cells are reported. E, Stomatal aperture widths of Pearson and *Nr* in response to ABA. Intact soil-grown tomato plants were treated with 5 μL L^{-1} ethylene gas for 24 h prior to the incubation of whole leaves under white light in a 20 μM ABA solution for 0 and 45 min. Averages ± SE of 90 stomata from three separate experiments are reported. Asterisks represent significant differences in DPBA, DCF, or stomatal aperture ($P < 0.001$) with and without ethylene treatment within a genotype, number signs represent significant differences ($P < 0.001$) between genotypes under similar treatments, and daggers represents significant differences in response to ABA within a genotype and ethylene treatment ($P < 0.001$). Statistics were determined using two-way ANOVA followed by Tukey's post hoc test. Bars = 5 μm.

and vacuole, but dye incompatibility and the absence of marker lines make inconclusive the analysis of this subcellular localization.

Flavonol accumulation in guard cells is consistent with prior reports examining guard cells of *Vicia faba* (Schnabl et al., 1986; Takahama, 1988) and Arabidopsis (Watkins et al., 2014; An et al., 2016). Localized accumulation of flavonols in guard cells may be the result of localized synthesis or localized transport of these molecules into the cells. Previous reports suggest that genes encoding two enzymes in the flavonoid biosynthetic pathway, CHS and FLS, are expressed in guard cells, but not surrounding pavement cells, of Arabidopsis using *CHS* promoter-GUS and GFP-FLS fusion proteins (Kuhn et al., 2011; Watkins et al., 2014). Additionally, the transcriptome of Arabidopsis guard cells includes transcripts for all the flavonol biosynthetic enzymes (Pandey et al., 2010). The localized accumulation of flavonols and their biosynthetic machinery in guard cells in multiple species suggests an important function of these molecules in this cell type.

To assess the function of flavonol antioxidants in guard cells, we used mutants with altered flavonol and anthocyanin accumulation. The predicted changes in accumulation of flavonols, based on the site of the mutation in the flavonol biosynthetic pathway, were detected in guard cells and leaves. We imaged flavonol accumulation in guard cells using the flavonol dye, DPBA, in two tomato anthocyanin mutants (Goldsbrough et al., 1994; Yoder et al., 1994). The levels of flavonols are either decreased or increased depending on whether the location of the mutated enzyme is before or after flavonol synthesis (Fig. 1), as demonstrated by DPBA staining of guard cells and LC-MS of leaf extracts. The *are* mutant has a lower abundance of flavonols than the wild type (Fig. 3; Table I), due to a mutation in the gene encoding the enzyme F3H, which is upstream of flavonol synthesis, while *aw* has higher kaempferol and quercetin accumulation, due to a mutation in the gene encoding the DFR enzyme, which is downstream of flavonol synthesis (Goldsbrough et al., 1994; Yoder et al., 1994; Maloney et al., 2014). Naringenin is not detected by DPBA (Lewis et al., 2011),

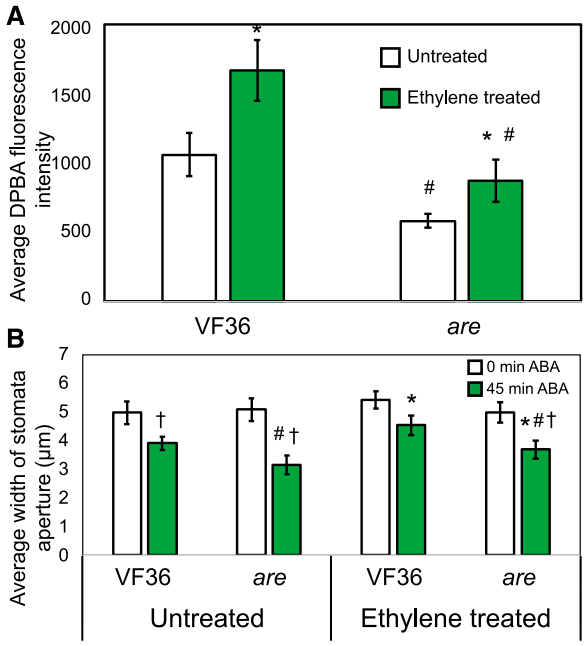

Figure 10. Ethylene treatment dampens ABA-induced stomatal closure through inducing flavonol accumulation in VF36 guard cells, with reduced responses in *are* guard cells. A, DPBA fluorescence in VF36 and *are* guard cells with and without treatment with 5 μL L^{-1} ethylene gas for 24 h visualized by LSCM. Averages and ± SE of DPBA fluorescence of 20 guard cells are reported. B, Stomatal aperture widths of VF36 and *are* in the absence and presence of 5 μL L^{-1} ethylene gas for 24 h prior to the incubation of whole leaves in 20 μM ABA for 0 and 45 min. Averages ± SE of 90 stomata from three separate experiments are reported. Statistics were determined using two-way ANOVA followed by Tukey's post hoc test with differences ($P < 0.01$) indicated. Asterisks indicate significant differences within genotypes with ethylene added, number signs indicate significant differences between genotypes under similar treatments, and daggers indicate significant differences between 0- and 45-min ABA treatment within a genotype and ethylene treatment.

but using LC-MS, it is evident that both the *are* and *aw* mutants had higher levels of the flavonol precursor naringenin, similar to roots and hypocotyls (Maloney et al., 2014). The agreement between these two methods indicates the presence of robust changes in flavonol levels in guard cells of these mutants and that DPBA fluorescence accurately reports flavonol accumulation, but with spatial resolution not possible by LC-MS.

To test the hypothesis that flavonols locally alter ROS in guard cells, thereby modulating stomatal aperture and leaf water exchange, we used DCF, a general ROS sensor, and PO1, an H_2O_2 selective sensor, to examine the effect of flavonol levels on ROS accumulation parallel to measurements of stomatal aperture. Confocal micrographs reveal DCF and PO1 fluorescence localized to guard cells but not surrounding pavement cells of wild-type leaves (Figs. 2, 4, and 5). This pattern of guard cell localization was similar to the DPBA fluorescence pattern, suggesting the intriguing possibility that the machinery for the synthesis of flavonols and ROS is developmentally coordinated and that flavonols may be acting in this tissue to modulate ROS. In light-grown untreated leaves, ROS homeostasis was examined in *are* guard cells, and the levels of DCF and PO1 fluorescence were elevated, consistent with the reduction in the flavonols quercetin and kaempferol. In contrast, the *aw* mutant, with increased flavonols, has reduced DCF signal. Both mutations elevated the level of the flavonol precursor naringenin, indicating that this molecule is not functioning to modulate ROS. The degree of guard cell closure was proportional to ROS sensor signal in these seedlings (Fig. 5). These findings extend a study of the flavonol-deficient *tt4* mutant in Arabidopsis, which also had elevated DCF fluorescence and enhanced guard cell closure (Watkins et al., 2014). The antioxidant glutathione also has been implicated in modulating ROS-induced stomatal closure, as mutations that impair its synthesis have elevated ROS and guard cell closure (Okuma et al., 2011; Munemasa et al., 2013). This study goes beyond these prior reports by utilizing a second tomato mutant with increased flavonols with the opposite response, reduced ROS and reduced guard cell aperture. As both of these mutants have elevated naringenin and reduced levels of anthocyanins, it is clear that flavonols, but not their precursors or downstream products, modulate this response.

To further test the role of flavonols in regulating guard cell signaling and stomatal aperture, these metabolites also were elevated by treatment of wild-type plants with ethylene. This treatment also resulted in decreased ROS sensor fluorescence and reduced stomatal closure (Fig. 9). This result mirrors the results with the *aw* mutant, which also has elevated flavonol levels, resulting in lower ROS signal and slower stomatal closure. In contrast, treatment of ethylene-insensitive *Nr* mutant plants, with a gain-of-function mutation in an ethylene receptor, rendering ethylene-insensitive plants (Lanahan et al., 1994; Yen et al., 1995; Clark et al., 1999; Negi et al., 2010), resulted in no change in flavonol levels, ROS, or stomatal aperture. To ask if ethylene modulation of ABA-induced stomatal closure requires flavonol induction, we examined the effects of ethylene on VF36 and the *are* mutant with reduced flavonols (Fig. 10). We found that ethylene-treated VF36 showed a 1.6-fold increase in flavonols, which were 1.9-fold higher than in the *are* mutant after the same treatment. Although ethylene-treated *are* stomata were more closed in response to ABA compared with wild-type stomata, ethylene appeared to slightly inhibit stomatal closure in this mutant. Consistent with this result, we also observed an increase in flavonol accumulation in *are* treated with ethylene. The absence of a mutant that produces no flavonols makes it difficult to demonstrate conclusively whether ethylene's inhibition of guard cells acts through flavonols. These results are consistent with an attenuation of the ethylene effect in a mutant with reduced flavonol accumulation.

The ethylene regulation of flavonol synthesis is consistent with previous results that showed that flavonol accumulation is increased in Arabidopsis roots after treatment with the ethylene precursor 1-aminocyclopropane-1-carboxylic acid (Buer et al., 2007; Lewis et al., 2011).

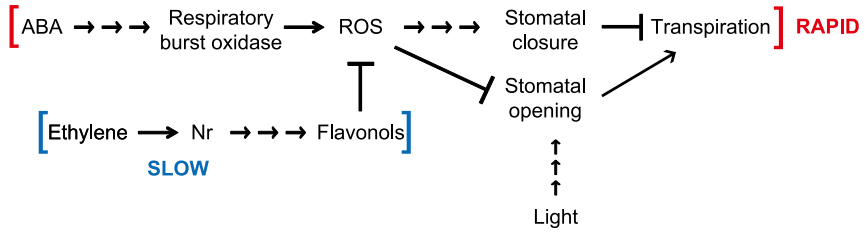

Figure 11. Proposed model of the effects of ABA-activated RBOH and ethylene-induced flavonols on stomatal movement. ABA is released into the cytosol, where it rapidly (within minutes) triggers respiratory burst oxidases, which induce a burst of ROS. ROS act as second messengers to signal stomatal closure, decreasing transpiration. Ethylene more slowly (within hours) induces flavonol accumulation in guard cells through the *Nr* receptor. Flavonols act as antioxidants to scavenge ROS and, thereby, inhibit stomatal closure. In *are*, which has less flavonol accumulation, guard cells have more ROS, faster stomatal closure rates in response to ABA, decreased water loss, and slower stomatal opening in response to light. The opposite is the case for guard cells of *aw*, which have elevated flavonol accumulation. Arrows represent activation, and bars represent repression

Auxin and ethylene promote flavonol synthesis (Buer et al., 2010) through inducing the transcript abundance of genes encoding flavonol biosynthetic enzymes (Lewis et al., 2011). Ethylene treatment or endogenous overproduction in *ethylene overproducing1* also drives flavonol synthesis in Arabidopsis guard cells, a response that is lost in the *ethylene insensitive2-5* mutant, resulting in lower ROS and less guard cell closure (Watkins et al., 2014).

The regulated synthesis of flavonols provides a mechanism for other guard cell responses. A recent study in tomato linked ethylene signaling with high humidity-induced stomatal opening (Arve and Torre, 2015). Ethylene treatment for 24 h increased conductance and stomatal aperture in moderate- and high-humidity conditions, while blocking the ethylene receptor or using the ethylene-insensitive mutant (*Nr*) reduced this stomatal opening response. Our results suggest that flavonol synthesis is an intermediate signal in this response. Induction of flavonol accumulation in Arabidopsis guard cells was observed after treatment with the plant growth regulator 5-aminolevulinic acid (An et al., 2016), which decreased ROS levels and ABA-induced stomatal closure. It is worth noting that some studies employing short-term ethylene treatments, which are too short for flavonol levels to be elevated, report enhanced closing of guard cells in *Arachis hypogea* and Arabidopsis (Pallas and Kays, 1982; Desikan et al., 2006; Ge et al., 2015), suggesting a second unlinked ethylene response in these guard cells. Together, these studies show that flavonols are regulated to modulate ROS signaling and guard cell aperture.

ABA-induced ROS bursts were modulated by flavonols in tomato leaves, with ROS accumulation preceding guard cell closure. The highest rate of increase in DCF fluorescence after ABA addition was detected in *are* guard cells, which accumulated less flavonols (Fig. 6). Additionally, *aw* guard cells showed the slowest rate of increased DCF fluorescence, linked to their higher flavonol accumulation. The rate of stomatal closure after 45 min in the presence of ABA is proportional to the level of ROS, consistent with this being a second messenger in controlling stomatal closure. This implies that, in tomato guard cells, flavonol levels are inversely related to ROS levels while ROS and stomatal closure rates are coordinated, both of which are consistent with flavonols acting as antioxidants in this cell type.

An important and previously unexplored question is whether flavonols affect light-dependent stomatal opening. Leaves were incubated in ABA in the dark for 3 h to close stomata completely (to a 1-μm aperture in all genotypes). Within 45 min after removal of ABA and transfer to light, there was a substantial 4-fold increase in aperture in the wild type (Fig. 7). The *are* mutant showed a reduced response (2.5-fold), while *aw* showed an enhanced response (5-fold change). Additionally, higher DCF fluorescence was observed in *are* guard cells and lower DCF fluorescence was observed in *aw* guard cells after light exposure, consistent with decreased and increased levels of flavonols and increased and decreased stomatal opening, respectively. This finding suggests the importance of flavonol accumulation in guard cells to facilitate rapid opening in the morning, which may facilitate CO_2 uptake and increased photosynthesis after sunrise.

To extend these results to the physiology of a whole leaf, we examined changes in leaf weight as a measure of transpiration. Because ABA-induced stomatal closure is the primary means by which plants respond to conditions of water stress (Leung and Giraudat, 1998), modulating the redox state in guard cells through altered flavonol synthesis would be expected to change transpiration rates. Consistent with this hypothesis, decreased flavonol levels in *are* leaves led to reduced water loss and increased flavonols in *aw* showed enhanced water loss compared with their parental lines (Fig. 8). Increased water loss also was observed in VF36 and *are* compared with AC and *aw*, which is likely linked to the greater stomatal density in the VF36 and *are* genotypes. A similar assay was employed to measure water loss from detached leaves, showing that the antioxidant ascorbic acid regulated stomatal closure in tobacco (*Nicotiana tabacum*; Chen and Gallie, 2004) and that ABA signaling in guard cells was modulated by glutathione (Munemasa et al., 2013). Together, these results indicate the function of small molecule antioxidants

to regulate transpiration rates by modulating ABA-dependent ROS signaling in guard cells.

We have constructed a model to synthesize these data, which is shown in Figure 11. This model outlines ABA-induced ROS increases via activated RBOH and their modulation by flavonols to control guard cell aperture. ABA is released into the cytosol, where it triggers respiratory burst oxidases, which induce a burst of ROS. ROS act as second messengers to signal stomatal closure and as inhibitors of light-induced stomatal opening to modulate gas exchange through guard cells. Flavonols act as antioxidants to scavenge ROS, thereby inhibiting stomatal closure, and their levels are regulated by ethylene. In *are*, which has less flavonol accumulation, guard cells have more ROS, resulting in faster stomatal closure rates in response to ABA, decreased water loss, and slower stomatal opening in response to light. In guard cells of *aw*, which have elevated flavonol accumulation, there is less ROS, decreased rates of stomatal closure in response to ABA, enhanced water loss, and increased stomatal opening in response to light.

CONCLUSION

This work extends our understanding of the mechanisms of flavonol actions in guard cells, providing insight into their role in an agricultural species and their mechanism of action. We found that ABA signaling through RBOH-produced ROS to induce stomatal closure is conserved in tomato, an important agricultural species. Better spatial resolution through our enhanced imaging technology showed complex subcellular accumulation patterns of flavonols, using DPBA fluorescence, and ROS, using DCF and PO1 fluorescence. Using mutants with altered flavonoid biosynthesis to manipulate the levels of flavonols in guard cells, both decreasing and increasing their abundance, modulates ROS levels and stomatal movement. Flavonol accumulation is increased by ethylene, which, in turn, modulates ROS accumulation and ABA-dependent guard cell closure. Together, these results indicate that flavonol levels affect ROS homeostasis, ABA-induced ROS, and stomatal closure as well as light-dependent stomatal opening. These changes in stomatal closure are linked to altered transpiration rates in detached leaves.

MATERIALS AND METHODS

Plant Growth and Ethylene Treatment

Tomato (*Solanum lycopersicum*) seeds used in these experiments include Pearson and *Nr* (Lanahan et al., 1994), VF36 and *are* (Yoder et al., 1994; Maloney et al., 2014), and AC and *aw* (Goldsbrough et al., 1994; Maloney et al., 2014) and were obtained from the Tomato Genetic Resource Center (http://tgrc.ucdavis.edu/). *Nr* seeds were generously provided by Harry Klee. Tomato seeds were germinated in Sunshine MVP RSi soil and placed in a 12-h-day growth chamber under 150 μmol m^{-2} s^{-1} cool-white light with relative humidity levels between 70% and 80% and grown for 4 to 5 weeks.

For ethylene treatments, 4- to 5-week-old wild-type and mutant plants were sealed in a plexiglass chamber to which ethylene gas was added to reach 5 μL L^{-1}. Control plants were placed in identical sealed containers without ethylene. After 24 h of incubation under 150 μmol m^{-2} s^{-1} cool-white light, leaves were excised and used for imaging DPBA or DCF fluorescence or in stomatal closure assays.

Visualization of Flavonol Accumulation Using DPBA

Individual leaves were excised and submerged in DPBA (Sigma-Aldrich; D9754) at 2.52 mg mL^{-1} containing 0.02% (v/v) Triton X-100 for 3 h. Whole leaves were then washed in deionized water for 1 min and mounted in deionized water between two coverslips. A Zeiss 880 LSCM apparatus was used to excite the leaf surfaces with 20% maximum laser power at 488 nm with a pinhole yielding 1 Airy Unit using LSCM settings that spectrally separated DPBA flavonol and chlorophyll fluorescence, using lambda scanning. DPBA fluorescence emission was collected between 475 and 619 nm (Lewis et al., 2011). Maximum intensity projections were produced from Z-stacks. The gain settings were selected to maximize the total flavonol signal while preventing oversaturation. All micrographs within each panel were acquired using identical offset, gain, and pinhole settings using the same detectors. Post-image quantification of DPBA fluorescence intensities was done using ZEN Black by placing a region of interest (ROI) around the nucleus of each guard cell and around an area in the cytosol with no chloroplasts present. The average intensity values within each ROI were recorded and averaged.

Analysis of Flavonoids by LC-MS

Flavonols were quantified in a method adapted from earlier publications (Maloney et al., 2014; Watkins et al., 2014). Three fully expanded leaves from each plant were collected from three plants of each genotype and flash frozen in liquid nitrogen; this was repeated three times on different sets of plants. Metabolites were extracted by first grinding the tissue and then using an acetone solvent with a 5 μM internal standard, formononetin. The samples were subjected to an acid hydrolysis to remove carbohydrates from the flavonol backbone, separated using an ethyl acetate phase separation, and dried down. Samples were stored at −80°C until suspended in acetone to be run on the mass spectrometer. Samples were analyzed on a Thermo LTQ Orbitrap XL with an electrospray ionization source, coupled to a Thermo Accela 1250 pump and autosampler (Thermo Fisher), using a Security Guard column in line with a Luna 150- × 3-mm C18 column, both from Phenomenex. For flavonol analysis, 10 μL of each sample was injected with a solvent of water: acetonitrile, both containing 0.1% (v/v) formic acid. The gradient is as follows: 90% (v/v) water:10% (v/v) acetonitrile to 10% (v/v) water:90% (v/v) acetonitrile in a time span of 18.5 min. From 18.5 to 20 min, the gradient moves from 10% (v/v) water:90% (v/v) acetonitrile back to 90% (v/v) water:10% (v/v) acetonitrile and holds at these concentrations for another 2 min to recondition the column. MS2 fragmentation spectra of flavonols were induced using 35-kV collision-induced dissociation. Absolute quantities of metabolites were found by comparing peak area data with standard curves created using pure standards of naringenin, quercetin, and kaempferol (Indofine Chemicals). As naringenin was at levels near the limit of detection, only samples with peaks greater than 2 times the background were used for quantification, to ensure accurate values. Spectra of samples were compared with those of standards and those listed on the MassBank database (www.massbank.jp). Data were analyzed by quantifying peak areas using Thermo Xcalibur software and with normalization to the internal standard formononetin (Indofine Chemicals).

DCF Imaging and Quantification

CM H_2DCF-DA, a generic ROS sensor (Halliwell and Whiteman, 2004), was dissolved in dimethyl sulfoxide to yield a 50 mM stock. This was diluted in deionized water to yield a final concentration of 6.25 μM with a final dimethyl sulfoxide concentration of 0.0125% (v/v). Epidermal strips were prepared by spraying a microscope slide with a silicone-based medical adhesive (Hollister; stock no. 7730). After 10 min, the basal epidermis of the leaf was gently pressed into the dried adhesive coat, and the leaf was gently scraped with a pipette tip until only the fixed epidermis remained (Young et al., 2006; Watkins et al., 2014). The epidermis was stained for 30 min with two drops of 6.25 μM CM H_2DCF-DA dye and washed with deionized water. A Zeiss 880 LSCM device was used to excite the leaf surfaces with 0.07% maximum laser power at 488 nm with a 3.5 digital gain. Settings were optimized to spectrally separate the fluorescence of DCF and chlorophyll, using lambda scanning. The DCF signal was

collected between 495 and 527 nm with a pinhole yielding 1 Airy Unit, making sure to limit excess exposure to the laser that induces ROS. Maximum intensity projections were produced from Z-stacks. All micrographs within each panel were acquired using identical offset, gain, and pinhole settings using the same detectors.

In Figures 2, 5, 6, and 7, DCF fluorescence was imaged using a Zeiss 880 LSCM device. DCF fluorescence intensities were measured using ZEN Black by placing an ROI around the whole guard cell. The average intensity values within each ROI were recorded and averaged. In Figures 5 and 9, DCF fluorescence was imaged using a Zeiss 710 LSCM device. DCF fluorescence intensities were measured using ZEN Black by placing an ROI around the nucleus of each guard cell and around the nonnuclear area with no chloroplasts present. The average intensity values within each ROI were recorded and averaged. Figure 5A shows confocal micrographs of DCF fluorescence in guard cells taken on a Zeiss 880 LSCM device, while the quantification values in Figure 5B are taken from the Zeiss 710 images from Supplemental Figure S4.

PO1 Imaging and Quantification

PO1, an H_2O_2 sensor (Lin et al., 2013; Liang et al., 2014), was dissolved in dimethyl sulfoxide to yield a 5 mM stock. This was diluted in deionized water to yield a final concentration of 33 μM. Epidermal strips were prepared as described above. The epidermis was stained for 30 min with two drops of 33 μM PO1 dye and washed with deionized water. A Zeiss 880 LSCM device was used to excite the leaf surfaces with 0.4% maximum laser power at 488 nm with a 2× digital gain. Settings were optimized to spectrally separate the fluorescence of DCF and chlorophyll, using lambda scanning. The DCF signal was collected between 495 and 527 nm with a pinhole yielding 1 Airy Unit, making sure to limit excess exposure to the laser that induces ROS. Maximum intensity projections were produced from Z-stacks. All micrographs within each panel were acquired using identical offset, gain, and pinhole settings using the same detectors. Total guard cell PO1 fluorescence intensities were measured using ZEN Black by placing an ROI around the whole guard cell. The average intensity values within each ROI were recorded and averaged. Subcellular PO1 fluorescence intensities were measured using ZEN Black by placing an ROI around the nucleus of each guard cell and around the nonnuclear area with no chloroplasts present.

Stomatal Opening and Closing Assays

ABA-induced stomatal closure assays were performed with plants 4 to 5 weeks after germination. Fully expanded leaves were excised and submerged in opening solution (5 μM KCl, 50 μM $CaCl_2$, and 10 μM MES buffer, pH 5.6) and incubated under cool-white light (150 μmol m^{-2} s^{-1}) for 3 h. To induce stomatal closure, leaves were transferred to a similar opening solution with 20 μM ABA added to induce closure (Jammes et al., 2009). After incubation in the ABA solution under white light for 0, 15, 30, or 45 min, leaf peels were prepared and imaged using bright-field imaging with a Zeiss Axio Zoom V16 microscope with an AxioCam HR R3 color camera (Jammes et al., 2009). Z-stacks were taken at 258× total magnification and compressed into a single extended depth-of-focus image. Apertures were measured using ImageJ software. To image the effects of ethylene on ABA-induced stomatal closure, plants were treated with ethylene gas for 24 h prior to the assay.

To induce stomatal opening, leaves were excised and placed in stomatal opening buffer containing 20 μM ABA and then placed in the dark for 3 h. Leaves were transferred to stomatal opening buffer without ABA and placed in the light for 0 or 45 min. The widths of stomatal apertures were quantified as above.

Leaf Water Loss Assay

Water loss from excised leaves was measured in fully expanded leaves that were detached from well-watered plants and immediately weighed, as adapted from Chen and Gallie (2004) and Munemasa et al. (2013). Water loss from detached leaves was followed by leaf weight every 5 min for 40 min. Four leaves from four separate plants were used in four separate experiments. The average percentage leaf weight loss was plotted over time.

Stomata Density Measurements

To quantify stomatal densities, epidermal peels were generated from the basal side of fully expanded leaves. Peels were imaged with differential interference contrast microscopy using a Zeiss Avio Zoom V16 at 100× magnification. Z-stacks were compressed into a single extended depth-of-focus image. Five areas per leaf were imaged from three leaves from three different plants for each genotype. Stomatal densities were reported as the number of stomata per 1.5 mm^2.

Statistical Analysis

The data for the fluorescence intensities of DPBA and DCF, the widths of stomatal apertures, and the leaf weight loss were analyzed by two-way ANOVA using GraphPad Prism 7, comparing within genotypes between different treatments and comparing between genotypes under similar treatments. Tukey's multiple comparison tests were then used to determine whether the differences between treatments within genotypes and the differences between genotypes within treatments were significant. LC-MS data and stomatal density were quantified using Student's *t* test in GraphPad Prism 7, comparing levels of a specific flavonol between a mutant and its respective background.

Accession Numbers

Sequence data for genes in this article can be found at https://solgenomics.net/ under the following accession numbers: F3H (Solyc02g083860, SGN-U563669), DFR (Solyc02g085020, SGN-U569072), and NR (Solyc09g075440, SGN-U580538).

Supplemental Data

The following supplemental materials are available.

Supplemental Figure S1. DPBA fluorescence and DCF fluorescence are localized to the nucleus.

Supplemental Figure S2. ROS accumulation pattern and colocalization analysis in guard cells in the AC genotype.

Supplemental Figure S3. DPBA fluorescence pattern in guard cells compared with a vacuole-specific stain in AC tomato leaves.

Supplemental Figure S4. DPBA and DCF fluorescence in guard cells visualized using a Zeiss LSM 710 confocal microscope.

ACKNOWLEDGMENTS

We thank Dr. Glen Marrs and Dr. Heather Brown-Harding for help with microscopy and Dr. Kim Nelson for help with LC-MS. We appreciate the helpful suggestions of Dr. Sarah Assmann and Dr. Leslie Poole in sharing ideas during the preparation of this article. The sharing of seeds by the Tomato Genetic Resource Center is greatly appreciated.

Received July 24, 2017; accepted October 17, 2017; published October 19, 2017.

LITERATURE CITED

Allen GJ, Chu SP, Schumacher K, Shimazaki CT, Vafeados D, Kemper A, Hawke SD, Tallman G, Tsien RY, Harper JF, et al (2000) Alteration of stimulus-specific guard cell calcium oscillations and stomatal closing in Arabidopsis det3 mutant. Science **289:** 2338–2342

Alvarez ME, Pennell RI, Meijer PJ, Ishikawa A, Dixon RA, Lamb C (1998) Reactive oxygen intermediates mediate a systemic signal network in the establishment of plant immunity. Cell **92:** 773–784

An Y, Feng X, Liu L, Xiong L, Wang L (2016) ALA-induced flavonols accumulation in guard cells is involved in scavenging H_2O_2 and inhibiting stomatal closure in Arabidopsis cotyledons. Front Plant Sci **7:** 1713

Apel K, Hirt H (2004) Reactive oxygen species: metabolism, oxidative stress, and signal transduction. Annu Rev Plant Biol **55:** 373–399

Arnaud D, Lee S, Takebayashi Y, Choi D, Choi J, Sakakibara H, Hwang I (2017) Cytokinin-mediated regulation of reactive oxygen species homeostasis modulates stomatal immunity in *Arabidopsis*. Plant Cell **29:** 543–559

Arve LE, Torre S (2015) Ethylene is involved in high air humidity promoted stomatal opening of tomato (*Lycopersicon esculentum*) leaves. Funct Plant Biol **42:** 376–386

Asada K (2006) Production and scavenging of reactive oxygen species in chloroplasts and their functions. Plant Physiol **141:** 391–396

Assmann SM, Jegla T (2016) Guard cell sensory systems: recent insights on stomatal responses to light, abscisic acid, and CO_2. Curr Opin Plant Biol **33:** 157–167

Ballester AR, Molthoff J, de Vos R, Hekkert BT, Orzaez D, Fernández-Moreno JP, Tripodi P, Grandillo S, Martin C, Heldens J, et al (2010) Biochemical and molecular analysis of pink tomatoes: deregulated expression of the gene encoding transcription factor SlMYB12 leads to pink tomato fruit color. Plant Physiol **152:** 71–84

Balmant KM, Zhang T, Chen S (2016) Protein phosphorylation and redox modification in stomatal guard cells. Front Physiol **7:** 26

Baxter A, Mittler R, Suzuki N (2014) ROS as key players in plant stress signalling. J Exp Bot **65:** 1229–1240

Blatt MR, Garcia-Mata C, Sokolovski S (2007) Membrane transport and Ca^{2+} oscillations in guard cells. *In* PDS Mancuso, DS Shabala, eds, Rhythms in Plants. Springer, Berlin, pp 115–133

Brown DE, Rashotte AM, Murphy AS, Normanly J, Tague BW, Peer WA, Taiz L, Muday GK (2001) Flavonoids act as negative regulators of auxin transport in vivo in *Arabidopsis*. Plant Physiol **126:** 524–535

Brown DI, Griendling KK (2009) Nox proteins in signal transduction. Free Radic Biol Med **47:** 1239–1253

Buer CS, Imin N, Djordjevic MA (2010) Flavonoids: new roles for old molecules. J Integr Plant Biol **52:** 98–111

Buer CS, Muday GK (2004) The *transparent testa4* mutation prevents flavonoid synthesis and alters auxin transport and the response of Arabidopsis roots to gravity and light. Plant Cell **16:** 1191–1205

Buer CS, Muday GK, Djordjevic MA (2007) Flavonoids are differentially taken up and transported long distances in Arabidopsis. Plant Physiol **145:** 478–490

Cervantes E (2001) ROS in root gravitropism: the auxin messengers? Trends Plant Sci **6:** 556

Chater C, Peng K, Movahedi M, Dunn JA, Walker HJ, Liang YK, McLachlan DH, Casson S, Isner JC, Wilson I, et al (2015) Elevated CO_2-induced responses in stomata require ABA and ABA signaling. Curr Biol **25:** 2709–2716

Chen Z, Gallie DR (2004) The ascorbic acid redox state controls guard cell signaling and stomatal movement. Plant Cell **16:** 1143–1162

Chen ZH, Hills A, Lim CK, Blatt MR (2010) Dynamic regulation of guard cell anion channels by cytosolic free Ca^{2+} concentration and protein phosphorylation. Plant J **61:** 816–825

Choudhury FK, Rivero RM, Blumwald E, Mittler R (2017) Reactive oxygen species, abiotic stress and stress combination. Plant J **90:** 856–867

Clark DG, Gubrium EK, Barrett JE, Nell TA, Klee HJ (1999) Root formation in ethylene-insensitive plants. Plant Physiol **121:** 53–60

Conklin PL, Williams EH, Last RL (1996) Environmental stress sensitivity of an ascorbic acid-deficient Arabidopsis mutant. Proc Natl Acad Sci USA **93:** 9970–9974

Desikan R, Last K, Harrett-Williams R, Tagliavia C, Harter K, Hooley R, Hancock JT, Neill SJ (2006) Ethylene-induced stomatal closure in Arabidopsis occurs via AtrbohF-mediated hydrogen peroxide synthesis. Plant J **47:** 907–916

Dickinson BC, Huynh C, Chang CJ (2010) A palette of fluorescent probes with varying emission colors for imaging hydrogen peroxide signaling in living cells. J Am Chem Soc **132:** 5906–5915

Farber M, Attia Z, Weiss D (2016) Cytokinin activity increases stomatal density and transpiration rate in tomato. J Exp Bot **67:** 6351–6362

Foreman J, Demidchik V, Bothwell JHF, Mylona P, Miedema H, Torres MA, Linstead P, Costa S, Brownlee C, Jones JD, et al (2003) Reactive oxygen species produced by NADPH oxidase regulate plant cell growth. Nature **422:** 442–446

Gayomba S, Watkins J, Muday G (2017) Flavonols regulate plant growth and development through regulation of auxin transport and cellular redox status. *In* K Yoshida, V Cheynier, S Quideau, eds, Recent Advances in Polyphenol Research. John Wiley & Sons, Chichester, UK, pp 143–170

Ge XM, Cai HL, Lei X, Zhou X, Yue M, He JM (2015) Heterotrimeric G protein mediates ethylene-induced stomatal closure via hydrogen peroxide synthesis in Arabidopsis. Plant J **82:** 138–150

Gilroy S, Białasek M, Suzuki N, Górecka M, Devireddy AR, Karpiński S, Mittler R (2016) ROS, calcium, and electric signals: key mediators of rapid systemic signaling in plants. Plant Physiol **171:** 1606–1615

Goldsbrough A, Belzile F, Yoder JI (1994) Complementation of the tomato anthocyanin without (aw) mutant using the dihydroflavonol 4-reductase gene. Plant Physiol **105:** 491–496

Halliwell B, Whiteman M (2004) Measuring reactive species and oxidative damage in vivo and in cell culture: how should you do it and what do the results mean? Br J Pharmacol **142:** 231–255

Hedrich R, Busch H, Raschke K (1990) Ca^{2+} and nucleotide dependent regulation of voltage dependent anion channels in the plasma membrane of guard cells. EMBO J **9:** 3889–3892

Heim KE, Tagliaferro AR, Bobilya DJ (2002) Flavonoid antioxidants: chemistry, metabolism and structure-activity relationships. J Nutr Biochem **13:** 572–584

Hichri I, Barrieu F, Bogs J, Kappel C, Delrot S, Lauvergeat V (2011) Recent advances in the transcriptional regulation of the flavonoid biosynthetic pathway. J Exp Bot **62:** 2465–2483

Hornberg C, Weiler E (1984) High-affinity binding sites for abscisic acid on the plasmalemma of *Vicia faba* guard cells. Nature **310:** 321–324

Inupakutika MA, Sengupta S, Devireddy AR, Azad RK, Mittler R (2016) The evolution of reactive oxygen species metabolism. J Exp Bot **67:** 5933–5943

Jammes F, Song C, Shin D, Munemasa S, Takeda K, Gu D, Cho D, Lee S, Giordo R, Sritubtim S, et al (2009) MAP kinases MPK9 and MPK12 are preferentially expressed in guard cells and positively regulate ROS-mediated ABA signaling. Proc Natl Acad Sci USA **106:** 20520–20525

Jezek M, Blatt MR (2017) The membrane transport system of the guard cell and its integration for stomatal dynamics. Plant Physiol **174:** 487–519

Jiang M, Zhang J (2002) Involvement of plasma-membrane NADPH oxidase in abscisic acid- and water stress-induced antioxidant defense in leaves of maize seedlings. Planta **215:** 1022–1030

Jiang M, Zhang J (2003) Cross-talk between calcium and reactive oxygen species originated from NADPH oxidase in abscisic acid-induced antioxidant defence in leaves of maize seedlings. Plant Cell Environ **26:** 929–939

Joo JH, Bae YS, Lee JS (2001) Role of auxin-induced reactive oxygen species in root gravitropism. Plant Physiol **126:** 1055–1060

Karpiński S, Szechyńska-Hebda M, Wituszyńska W, Burdiak P (2013) Light acclimation, retrograde signalling, cell death and immune defences in plants. Plant Cell Environ **36:** 736–744

Kuhn BM, Geisler M, Bigler L, Ringli C (2011) Flavonols accumulate asymmetrically and affect auxin transport in Arabidopsis. Plant Physiol **156:** 585–595

Kwak JM, Mori IC, Pei ZM, Leonhardt N, Torres MA, Dangl JL, Bloom RE, Bodde S, Jones JD, Schroeder JI (2003) NADPH oxidase AtrbohD and AtrbohF genes function in ROS-dependent ABA signaling in Arabidopsis. EMBO J **22:** 2623–2633

Lanahan MB, Yen HC, Giovannoni JJ, Klee HJ (1994) The never ripe mutation blocks ethylene perception in tomato. Plant Cell **6:** 521–530

Lee S, Choi H, Suh S, Doo IS, Oh KY, Choi EJ, Schroeder Taylor AT, Low PS, Lee Y (1999) Oligogalacturonic acid and chitosan reduce stomatal aperture by inducing the evolution of reactive oxygen species from guard cells of tomato and *Commelina communis*. Plant Physiol **121:** 147–152

Lepiniec L, Debeaujon I, Routaboul JM, Baudry A, Pourcel L, Nesi N, Caboche M (2006) Genetics and biochemistry of seed flavonoids. Annu Rev Plant Biol **57:** 405–430

Leshem Y, Seri L, Levine A (2007) Induction of phosphatidylinositol 3-kinase-mediated endocytosis by salt stress leads to intracellular production of reactive oxygen species and salt tolerance. Plant J **51:** 185–197

Leung J, Giraudat J (1998) Abscisic acid signal transduction. Annu Rev Plant Physiol Plant Mol Biol **49:** 199–222

Lewis DR, Ramirez MV, Miller ND, Vallabhaneni P, Ray WK, Helm RF, Winkel BSJ, Muday GK (2011) Auxin and ethylene induce flavonol accumulation through distinct transcriptional networks. Plant Physiol **156:** 144–164

Li N, Sun L, Zhang L, Song Y, Hu P, Li C, Hao FS (2015) AtrbohD and AtrbohF negatively regulate lateral root development by changing the localized accumulation of superoxide in primary roots of Arabidopsis. Planta **241:** 591–602

Liang D, White RG, Waterhouse PM (2014) Mobile gene silencing in Arabidopsis is regulated by hydrogen peroxide. PeerJ **2:** e701

Lin VS, Dickinson BC, Chang CJ (2013) Boronate-based fluorescent probes: imaging hydrogen peroxide in living systems. Methods Enzymol **526:** 19–43

Ma Y, Szostkiewicz I, Korte A, Moes D, Yang Y, Christmann A, Grill E (2009) Regulators of PP2C phosphatase activity function as abscisic acid sensors. Science **324:** 1064–1068

Maloney GS, DiNapoli KT, Muday GK (2014) The anthocyanin reduced tomato mutant demonstrates the role of flavonols in tomato lateral root and root hair development. Plant Physiol **166:** 614–631

McAinsh MR, Clayton H, Mansfield TA, Hetherington AM (1996) Changes in stomatal behavior and guard cell cytosolic free calcium in response to oxidative stress. Plant Physiol **111:** 1031–1042

McCourt P, Creelman R (2008) The ABA receptors: we report you decide. Curr Opin Plant Biol **11:** 474–478

Minguet-Parramona C, Wang Y, Hills A, Vialet-Chabrand S, Griffiths H, Rogers S, Lawson T, Lew VL, Blatt MR (2016) An optimal frequency in Ca^{2+} oscillations for stomatal closure is an emergent property of ion transport in guard cells. Plant Physiol **170:** 33–42

Mittler R (2002) Oxidative stress, antioxidants and stress tolerance. Trends Plant Sci **7:** 405–410

Mittler R, Blumwald E (2015) The roles of ROS and ABA in systemic acquired acclimation. Plant Cell **27:** 64–70

Müller K, Carstens AC, Linkies A, Torres MA, Leubner-Metzger G (2009) The NADPH-oxidase AtrbohB plays a role in Arabidopsis seed afterripening. New Phytol **184:** 885–897

Munemasa S, Muroyama D, Nagahashi H, Nakamura Y, Mori IC, Murata Y (2013) Regulation of reactive oxygen species-mediated abscisic acid signaling in guard cells and drought tolerance by glutathione. Front Plant Sci **4:** 472

Mustilli AC, Merlot S, Vavasseur A, Fenzi F, Giraudat J (2002) Arabidopsis OST1 protein kinase mediates the regulation of stomatal aperture by abscisic acid and acts upstream of reactive oxygen species production. Plant Cell **14:** 3089–3099

Negi S, Sukumar P, Liu X, Cohen JD, Muday GK (2010) Genetic dissection of the role of ethylene in regulating auxin-dependent lateral and adventitious root formation in tomato. Plant J **61:** 3–15

Okuma E, Jahan MS, Munemasa S, Hossain MA, Muroyama D, Islam MM, Ogawa K, Watanabe-Sugimoto M, Nakamura Y, Shimoishi Y, et al (2011) Negative regulation of abscisic acid-induced stomatal closure by glutathione in Arabidopsis. J Plant Physiol **168:** 2048–2055

Orman-Ligeza B, Parizot B, de Rycke R, Fernandez A, Himschoot E, Van Breusegem F, Bennett MJ, Périlleux C, Beeckman T, Draye X (2016) RBOH-mediated ROS production facilitates lateral root emergence in *Arabidopsis*. Development **143:** 3328–3339

Osaki T, Uchida Y, Hirayama J, Nishina H (2011) Diphenyleneiodonium chloride, an inhibitor of reduced nicotinamide adenine dinucleotide phosphate oxidase, suppresses light-dependent induction of clock and DNA repair genes in zebrafish. Biol Pharm Bull **34:** 1343–1347

Pallas JE, Kays SJ (1982) Inhibition of photosynthesis by ethylene: a stomatal effect. Plant Physiol **70:** 598–601

Pandey S, Wang RS, Wilson L, Li S, Zhao Z, Gookin TE, Assmann SM, Albert R (2010) Boolean modeling of transcriptome data reveals novel modes of heterotrimeric G-protein action. Mol Syst Biol **6:** 372

Park SY, Fung P, Nishimura N, Jensen DR, Fujii H, Zhao Y, Lumba S, Santiago J, Rodrigues A, Chow TF, et al (2009) Abscisic acid inhibits type 2C protein phosphatases via the PYR/PYL family of START proteins. Science **324:** 1068–1071

Peer WA, Brown DE, Tague BW, Muday GK, Taiz L, Murphy AS (2001) Flavonoid accumulation patterns of *transparent testa* mutants of Arabidopsis. Plant Physiol **126:** 536–548

Pei ZM, Murata Y, Benning G, Thomine S, Klüsener B, Allen GJ, Grill E, Schroeder JI (2000) Calcium channels activated by hydrogen peroxide mediate abscisic acid signalling in guard cells. Nature **406:** 731–734

Poole LB, Karplus PA, Claiborne A (2004) Protein sulfenic acids in redox signaling. Annu Rev Pharmacol Toxicol **44:** 325–347

Poole LB, Nelson KJ (2008) Discovering mechanisms of signaling-mediated cysteine oxidation. Curr Opin Chem Biol **12:** 18–24

Rice-Evans C, Miller N, Paganga G (1997) Antioxidant properties of phenolic compounds. Trends Plant Sci **2:** 152–159

Sandalio LM, Romero-Puertas MC (2015) Peroxisomes sense and respond to environmental cues by regulating ROS and RNS signalling networks. Ann Bot **116:** 475–485

Saslowsky DE, Warek U, Winkel BSJ (2005) Nuclear localization of flavonoid enzymes in Arabidopsis. J Biol Chem **280:** 23735–23740

Schnabl H, Weissenbock G, Scharf H (1986) In vivo-microspectrophotometric characterization of flavonol glycosides in Vicia faba guard and epidermal cells. J Exp Bot **37:** 61–72

Schroeder JI, Hagiwara S (1990) Repetitive increases in cytosolic Ca^{2+} of guard cells by abscisic acid activation of nonselective Ca^{2+} permeable channels. Proc Natl Acad Sci USA **87:** 9305–9309

Sharma P, Jha AB, Dubey RS, Pessarakli M (2012) Reactive oxygen species, oxidative damage, and antioxidative defense mechanism in plants under stressful conditions. J Bot **2012:** e217037

Shi K, Li X, Zhang H, Zhang G, Liu Y, Zhou Y, Xia X, Chen Z, Yu J (2015) Guard cell hydrogen peroxide and nitric oxide mediate elevated CO^2-induced stomatal movement in tomato. New Phytol **208:** 342–353

Sierla M, Waszczak C, Vahisalu T, Kangasjärvi J (2016) Reactive oxygen species in the regulation of stomatal movements. Plant Physiol **171:** 1569–1580

Singh R, Parihar P, Singh S, Mishra RK, Singh VP, Prasad SM (2017) Reactive oxygen species signaling and stomatal movement: current updates and future perspectives. Redox Biol **11:** 213–218

Singh R, Singh S, Parihar P, Mishra RK, Tripathi DK, Singh VP, Chauhan DK, Prasad SM (2016) Reactive oxygen species (ROS): beneficial companions of plants' developmental processes. Front Plant Sci **7:** 1299

Steinhorst L, Kudla J (2013) Calcium and reactive oxygen species rule the waves of signaling. Plant Physiol **163:** 471–485

Suhita D, Raghavendra AS, Kwak JM, Vavasseur A (2004) Cytoplasmic alkalization precedes reactive oxygen species production during methyl jasmonate- and abscisic acid-induced stomatal closure. Plant Physiol **134:** 1536–1545

Suzuki N, Koussevitzky S, Mittler R, Miller G (2012) ROS and redox signalling in the response of plants to abiotic stress. Plant Cell Environ **35:** 259–270

Suzuki N, Miller G, Morales J, Shulaev V, Torres MA, Mittler R (2011) Respiratory burst oxidases: the engines of ROS signaling. Curr Opin Plant Biol **14:** 691–699

Swanson S, Gilroy S (2010) ROS in plant development. Physiol Plant **138:** 384–392

Swanson SJ, Choi WG, Chanoca A, Gilroy S (2011) In vivo imaging of Ca^{2+}, pH, and reactive oxygen species using fluorescent probes in plants. Annu Rev Plant Biol **62:** 273–297

Takahama U (1988) Oxidation of flavonols by hydrogen peroxide in epidermal and guard cells of *Vicia faba* L. Plant Cell Physiol **29:** 433–438

Tattini M, Galardi C, Pinelli P, Massai R, Remorini D, Agati G (2004) Differential accumulation of flavonoids and hydroxycinnamates in leaves of *Ligustrum vulgare* under excess light and drought stress. New Phytol **163:** 547–561

Van Breusegem F, Dat JF (2006) Reactive oxygen species in plant cell death. Plant Physiol **141:** 384–390

Wang Y, Chen ZH, Zhang B, Hills A, Blatt MR (2013) PYR/PYL/RCAR abscisic acid receptors regulate K^+ and Cl^- channels through reactive oxygen species-mediated activation of Ca^{2+} channels at the plasma membrane of intact Arabidopsis guard cells. Plant Physiol **163:** 566–577

Watkins JM, Hechler PJ, Muday GK (2014) Ethylene-induced flavonol accumulation in guard cells suppresses reactive oxygen species and moderates stomatal aperture. Plant Physiol **164:** 1707–1717

Willems P, Mhamdi A, Stael S, Storme V, Kerchev P, Noctor G, Gevaert K, Van Breusegem F (2016) The ROS wheel: refining ROS transcriptional footprints. Plant Physiol **171:** 1720–1733

Winkel-Shirley B (2001) Flavonoid biosynthesis: a colorful model for genetics, biochemistry, cell biology, and biotechnology. Plant Physiol **126:** 485–493

Winkel-Shirley B (2002) Biosynthesis of flavonoids and effects of stress. Curr Opin Plant Biol **5:** 218–223

Wu X, Qiao Z, Liu H, Acharya BR, Li C, Zhang W (2017) CML20, an Arabidopsis calmodulin-like protein, negatively regulates guard cell ABA signaling and drought stress tolerance. Front Plant Sci **8:** 824

Xia XJ, Gao CJ, Song LX, Zhou YH, Shi K, Yu JQ (2014) Role of H_2O_2 dynamics in brassinosteroid-induced stomatal closure and opening in *Solanum lycopersicum*. Plant Cell Environ **37:** 2036–2050

Yen HC, Lee S, Tanksley SD, Lanahan MB, Klee HJ, Giovannoni JJ (1995) The tomato Never-ripe locus regulates ethylene-inducible gene expression and is linked to a homolog of the Arabidopsis ETR1 gene. Plant Physiol **107:** 1343–1353

Yi C, Yao K, Cai S, Li H, Zhou J, Xia X, Shi K, Yu J, Foyer CH, Zhou Y (2015) High atmospheric carbon dioxide-dependent alleviation of salt stress is linked to RESPIRATORY BURST OXIDASE 1 (RBOH1)-dependent H_2O_2 production in tomato (*Solanum lycopersicum*). J Exp Bot **66:** 7391–7404

Yoder JI, Belzile F, Tong Y, Goldsbrough A (1994) Visual markers for tomato derived from the anthocyanin biosynthetic pathway. Euphytica **79:** 163–167

Yoshida R, Hobo T, Ichimura K, Mizoguchi T, Takahashi F, Aronso J, Ecker JR, Shinozaki K (2002) ABA-activated SnRK2 protein kinase is required for dehydration stress signaling in Arabidopsis. Plant Cell Physiol **43:** 1473–1483

Young JJ, Mehta S, Israelsson M, Godoski J, Grill E, Schroeder JI (2006) CO_2 signaling in guard cells: calcium sensitivity response modulation, a Ca^{2+}-independent phase, and CO_2 insensitivity of the gca2 mutant. Proc Natl Acad Sci USA **103:** 7506–7511